Corrosão & Proteção
Revista da Associação Brasileira de Corrosão • ISSN 0100-1485 • Ciência e Tecnologia em Corrosão
Ano 18 | nº 75 | set/out/nov/dez 2021

O futuro será ainda melhor

A nossa associação tem superado diversas crises durante sua história e hoje está mais forte do que nunca.

ABRACO
ASSOCIAÇÃO BRASILEIRA DE CORROSÃO

Expediente

A **Revista Corrosão & Proteção** é uma publicação oficial da ABRACO – Associação Brasileira de Corrosão, fundada em 17 de outubro de 1968.

ISSN 0100-1485

ABRACO
ASSOCIAÇÃO BRASILEIRA DE CORROSÃO

Nesta edição

Abraco mais forte do que nunca

Após um curso de corrosão com o Prof. Vicente Gentil, vários participantes, que consideramos pioneiros, entusiasmados com o tema, questionaram-se, o curso termina e nós não discutiremos mais o assunto?

O tempo passou, era o final do ano de 1968, um ano politicamente conturbado, quando os mesmos pioneiros, cabendo citar: Eng. Aldo cordeiro Dutra, Empresário Aldo Maestrelli, Professor Vicente Gentil, dentre outros, durante um seminário de inspeção de equipamento realizado pelo Instituto Brasileiro do Petróleo (IBP), decidiram pela criação de uma Associação para congregar profissionais, entidades e empresas devotadas ao estudo e combate à corrosão e, assim, no dia 18 de outubro do ano de 1968 foi assinada a ata de criação da Associação Brasileira de Corrosão – ABRACO.

O início foi difícil, sem sede própria, a ABRACO foi abrigada inicialmente no IBP, em seguida no Instituto Nacional de Tecnologia (INT), até que entra em cena um personagem muito importante na vida da ABRACO – Walter Marques da Silva, que atuou como Secretário Executivo por cerca de trinta anos. O Sr. Walter, como o chamávamos, deu uma enorme contribuição à Associação inclusive com a compra da sede própria onde a ABRACO está instalada até hoje.

Nos anos subsequentes à fundação, a Associação cresceu muito e passou por momentos muito bons financeiramente e por momentos mais delicados, porém nunca deixou de cumprir os seus objetivos. Realizou uma quantidade expressiva de eventos, entre congressos, seminários, mesas redondas, dentre outros. Realizou ainda centenas de cursos com milhares de participantes. Implantou a certificação de pessoas e criou o comitê Brasileiro de Normalização em Corrosão na ABNT. Estabeleceu parcerias com entidade importantes do país.

Nos cinquenta e três anos, passaram pela Associação centenas de colaboradores entre diretorias, professores, membros de comissões técnicas e outros voluntários que dedicaram o seu precioso tempo a uma causa comum, o combate à corrosão.

Ao final dos anos 1990, a ABRACO experimentou uma grande crise, na qual muitos não acreditavam na sua sobrevivência, no entanto ela resistiu e se tornou novamente muito forte até 2015. Nos últimos oito anos, a Associação passou outra vez por muitas dificuldades sendo elas financeiras, por conta de uma grave crise econômica no país e também devido à concorrência de entidades internacionais. Esta crise se agravou com a pandemia do coronavírus e mais uma vez a ABRACO resistiu, recuperou as finanças, realizou o Congresso Internacional de Corrosão e selou um excelente acordo com o ICorr.

Portanto, ela está mais forte do que nunca e certamente o futuro será muito melhor.

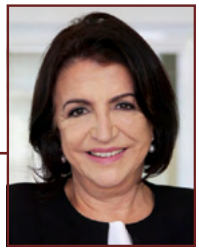

Zehbour Panossian
Presidente da ABRACO

GRANDES NOMES DA CORROSÃO

Passado, presente e futuro

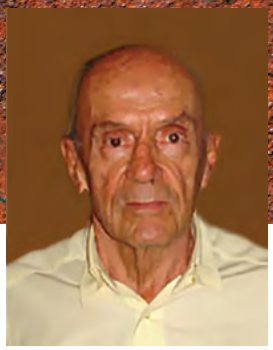

Vicente Gentil

Aldo Cordeiro Dutra

Zehbour Panossian

Neusvaldo Lira de Almeida

Nesta edição da revista Corrosão e Proteção vamos rever quatro nomes que foram considerados em edições anteriores. Homenagearemos dois fundadores da ABRACO e ressaltaremos a importância de dois nomes da atualidade, responsáveis pelo soerguimento da Associação – a presidente atual e o futuro presidente.

O passado

Era o ano de 1968 e dois grandes expoentes da corrosão fundaram a ABRACO: Prof. Vicente Gentil e o Eng. Aldo Cordeiro.

Prof. Vicente Gentil – O patrono da corrosão no Brasil

Vicente Gentil foi um grande professor universitário brasileiro e estudioso da química e eletroquímica, especialmente nos aspectos ligados à corrosão e à proteção anticorrosiva, com uma inigualável capacidade de comunicação. Foi o profissional que desenvolveu no país o interesse pela corrosão, tendo concebido e realizado os primeiros cursos de corrosão abertos à sociedade brasileira.

É de sua autoria o primeiro livro de corrosão do Brasil – atualmente na 6ª edição. A sua extrema capacidade de comunicação e dedicação impactou profundamente os conceitos e os estudos da corrosão em nossa terra.

O Professor Vicente Gentil nasceu no Rio de Janeiro, na zona norte da cidade, no dia 11 de setembro de 1928.

Aldo Cordeiro Dutra – Fundador da ABRACO e responsável pelo desenvolvimento da proteção catódica no Brasil

Aldo Cordeiro Dutra é um engenheiro brasileiro e estudioso da inspeção de equipamentos, da metrologia, da corrosão e particularmente da

proteção anticorrosiva, pelo uso da proteção catódica, com inigualável capacidade de trabalho e de visão de futuro. Foi o profissional que desenvolveu no país o interesse pela proteção catódica, tendo concebido e implantado a Associação Brasileira de Corrosão (ABRACO), juntamente com o Prof. Vicente Gentil, Aldo Maestrelli e outros.

É de sua autoria o primeiro livro de Proteção Catódica do Brasil juntamente com Laerce de Paula Nunes – atualmente na 5ª edição. A sua extrema capacidade de trabalho, determinação e dedicação aos interesses coletivos impactou profundamente os conceitos e os estudos da corrosão em nosso país. O Eng. Aldo Dutra nasceu em 25/11/1929, em Vila de Assunção, no município de Itapipoca, Estado do Ceará.

Nota: Lamentavelmente estes dois gigantes da corrosão não estão mais entre nós.

O presente

No ano de 2018, diante de uma grave recessão econômica do país, foi eleita para Presidente da ABRACO no biênio 2021 e 2022 a Profa. e Pesquisadora Zehbour Panassian, cuja missão seria recuperar a ABRACO juntamente com a Presidente da época Dra. Olga Baptista Ferraz e realizar o Congresso Internacional de Corrosão no Brasil. Ela tem cumprido a missão com maestria.

Dra. Zehbour Panossian – Uma das mais importantes pesquisadoras da corrosão no Brasil

Dra. Zehbour Panossian é uma eminente professora universitária e pesquisadora brasileira, estudiosa da corrosão e da eletroquímica, com toda uma vida dedicada à corrosão e à proteção anticorrosiva, com uma inigualável capacidade de trabalho e de comunicação.

Tem sido uma profissional motivadora do interesse pela pesquisa da corrosão no País, tendo concebido e realizado inúmeros cursos na Universidade de São Paulo e disponibilizado para a comunidade um grande acervo de trabalhos técnico-científicos, merecendo destaque o seu livro Corrosão e Proteção contra Corrosão em Equipamentos e Estruturas Metálicas.

A Dra. Zehbour pertence a uma família de origem armênia, mas nasceu em Beirute, no Líbano, na década de 1950. Veio para o Brasil, radicando-se na cidade de São Paulo, ainda pequena, na companhia dos seus pais e aqui adotou a nacionalidade brasileira.

O futuro

No ano de 2020, diante ainda da recessão econômica e de uma pandemia, foi eleito para Presidente da ABRACO no biênio 2023 e 2024 o Pesquisador Neusvaldo Lira de Almeida, cuja missão será continuar a recuperação da ABRACO juntamente com a Presidente atual Dra. Zehbour e justificar a afirmativa de que a ABRACO está mais forte do que nunca.

Pesquisador Neusvaldo Lira de Almeida

O Pesquisador Neusvaldo Lira de Almeida nasceu em Feira Grande no estado de Alagoas no dia 20/12/1955. Fez seus estudos fundamentais em Maceió, AL.

A entrada do Pesquisador Neusvaldo na pesquisa foi como ele mesmo relata, para nossa inteira sorte, absolutamente acidental:

"A minha iniciação em corrosão foi uma daquelas coisas que acontecem por acaso. As necessidades vão de certa forma direcionando, e você acaba escolhendo de acordo com algumas circunstâncias".

O entusiasmo do Neusvaldo pela pesquisa só se fez crescer ao longo do tempo. Vejamos o que afirma numa reflexão para a Revista Corrosão e Proteção:

"Em geral, a gente conhece bem uma parte do caminho; a outra se constrói enquanto caminha".

Neusvaldo: o futuro da ABRACO está em suas mãos – desejamos muita sorte e sucesso.

ABRACO mais forte do que nunca

O Brasil já vivia uma situação econômica adversa quando, há pouco mais de dois anos, a Organização Mundial da Saúde (OMS) decretou a pandemia de Covid-19. O isolamento social, necessário para conter a disseminação do novo coronavírus, tornou ainda mais difícil a sobrevivência de empresas e instituições.
E quando o país começava a se reerguer, ainda que lentamente, a guerra entre Rússia e Ucrânia deixou o cenário nebuloso mais uma vez.

"Estamos vivendo tempos conturbados", admite a presidente da ABRACO, Zehbour Panossian. "Além da pandemia, que deu um susto enorme em todos, vivemos problemas políticos jamais vistos, instabilidade econômica e ideológica internacional e, nos últimos meses, a invasão da Ucrânia. Enfrentar tudo isso é tarefa quase impossível."

Mas Panossian, com o apoio da diretoria e dos colaboradores da ABRACO, enfrentou – e a entidade segue firme em sua missão de difundir e desenvolver o conhecimento da corrosão e da proteção anticorrosiva. Só que, para permanecer de pé, foi preciso se adaptar.

A resposta à crise econômica pré-pandemia demandou a adequação da equipe a uma realidade de receitas reduzidas. A ABRACO, por exemplo, prescindiu de um gerente-geral e reduziu ao mínimo operacional o número de colaboradores em cada setor.

No ano seguinte, a pandemia demandou novos ajustes. Uma das primeiras alterações

Zehbour Panossian

foi a troca do trabalho presencial, na sede da Associação, pelo *home office*. Com o treinamento de colaboradores e instrutores para ministrar aulas virtuais, foi possível manter o ritmo dos cursos de pintura industrial nível 1 e lançar rodadas de palestras de variados temas de corrosão.

"A combinação de uma diretoria coesa e uma equipe competente e afinada com os objetivos da ABRACO foi o principal fator para enfrentarmos a crise econômica e os tempos de pandemia", acredita a diretora Olga Ferraz, que era presidente da Associação em 2019.

"Tivemos um diferencial muito importante: toda a equipe da ABRACO estava motivada para mudar a chave. Foi uma colaboração enorme que me surpreendeu positivamente. A terra estava fértil, já tinha sido adubada pela presidente anterior, era preciso semear", acrescenta Panossian.

Passo a passo

A atual presidente ressalta que o soerguimento da ABRACO se deu por etapas, sempre com muito diálogo. No início da pandemia, a diretoria mantinha reuniões semanais com inspetores de pintura, instrutores, pessoal de operação e demais colaboradores. Hoje, os encontros são quinzenais.

"Colhemos sugestões, estudamos normas e procedimentos e reorientamos as atividades tendo um foco: a ABRACO tinha que 'facilitar' a vida dos profissionais dedicados à corrosão. Precisávamos atendê-los com rapidez e eficiência", lembra Panossian.

Duas ações importantes nesse sentido, segundo ela, foram a disponibilização de aparelhos celulares para quase todos os colaboradores, a fim de agilizar o atendimento telefônico, e a criação do canal "Reclame aqui".

"Se o nosso apoio aos profissionais tinha entraves, precisávamos trabalhar para desatar nós e encontrar soluções. A expressão 'não pode' mudou para 'vamos ver o que pode ser feito'", relata.

Experiências anteriores

Zehbour Panossian e Olga Ferraz não foram as primeiras dirigentes a enfrentar momentos adversos. Laerce de Paula Nunes, presidente da ABRACO nos biênios 1999/2000 e 2009/2010, encontrou o país em recessão quando reassumiu o cargo, em 2017. Ele recorda as dificuldades de lidar com a crise econômica pouco tempo depois do boom econômico brasileiro.

"O maior desafio na minha gestão foi mudar a cultura", observa. "Quando se vive em ocasiões de abundância, acostuma-se a gastar mais e a não pensar em como empregar os recursos. A ABRACO havia crescido muito e foi doloroso ter que encolher."

Presidente na gestão anterior a de Nunes, Denise Souza de Freitas viu a crise nascer. Em meio ao aumento do desemprego e ao fim dos investimentos das empresas na capacitação de funcionários, as receitas da ABRACO, sobretudo as destinadas a cursos e acreditação, caíram drasticamente.

"Como forma de minimizar os efeitos da crise, tivemos que fazer um grande esforço para

Olga Ferraz

melhorar nossos processos internos", relembra Freitas. "Para isso, investimos para tornar a estrutura organizacional e financeira da ABRACO mais eficiente, mais próxima da realidade de uma empresa. Por exemplo, houve a implementação de ferramentas que nos permitiram acompanhar o andamento econômico-financeiro da Associação, com a adoção de um sistema informatizado para lançamentos contábeis, e foi introduzida como prática de gestão o uso da planilha DER – Demonstrativo de Resultados, para o controle e a previsão orçamentária."

Além disso, complementa a ex-presidente, a ABRACO firmou novos convênios e parcerias, bem como buscou formatos inovadores para os eventos promovidos pela Associação, de forma a reduzir custos e aumentar a participação de profissionais da área na organização. Freitas cita como exemplo o Congresso Internacional de Corrosão (INTERCORR) 2016, realizado em Búzios (RJ), com a presença de mais de 400 técnicos do Brasil e do exterior.

Laerce de Paula Nunes

Denise Freitas

Fé e resiliência

Presidentes em épocas distintas, os gestores ouvidos pela **Corrosão & Proteção** têm em comum a fé inabalável na instituição.

Laerce Nunes enaltece a força e a abrangência da marca ABRACO, que renderam o apoio de grandes empresas, universidades e centros de pesquisa. Denise Freitas, por sua vez, salienta que a Associação, mesmo após um longo período de paralisação devido à pandemia, permanece atuante e reconhecida por seus pares.

Já Olga Ferraz frisa que a atuação da ABRACO na formação de profissionais especializados e na organização de cursos, palestras e congressos é da maior relevância para a comunidade de corrosão.

Por fim, a atual presidente, Zehbour Panossian, enaltece a capacidade que a instituição sempre mostrou de não apenas resistir às adversidades, como também de sair mais fortalecido de cada crise.

"A história mostra que a ABRACO é resiliente. A ABRACO é forte!", afirma.

Agenda de eventos

EVENTO	LOCAL	DATA
Rodada de Palestras Técnicas (gratuita) O que é e o que fazer com as patentes	Online	08 de junho
Minievento: Sais em Superfícies a serem pintadas * Conta pontos no método de crédito estruturado.	Online	22 de junho
Minievento: Sistemas de Proteção Catódica * Conta pontos no método de crédito estruturado.	Online	27 de julho
Rodada de Palestras Técnicas (gratuita) Aspectos Relevantes do Recozimento e Decapagem dos Aços Inoxidáveis	Online	17 de agosto
Rodada de Palestras Técnicas (gratuita) Sistema de Pintura para Manutenção Offshore	Online	14 de setembro

PARTICIPE!

MAIS INFORMAÇÕES E INSCRIÇÕES NO SITE DA ABRACO:
WWW.ABRACO.ORG.BR

A cooperação entre ICorr e ABRACO

Isaac Catran, Florentina Melo (ABRACO) e Lúcia Fullalove (ICorr)

Adaptação do artigo publicado no Corrosion Management, a Revista do ICorr (Instituto de Corrosão do Reino Unido) de Março/ Abril 2022.

O curso de conversão para Inspetor de Pintura ICorr já é uma realidade e, à medida em que a ABRACO se aproxima para disponibilizar o curso do ICATS[1], gostaríamos de levar os leitores a conhecer a jornada percorrida até agora.

Foi em maio de 2018, durante o INTERCORR em São Paulo, Brasil, que a equipe técnica da ABRACO, Florentina (Flor) Melo e Isaac Catran se reuniram com Lúcia Fullalove. Na época Flor e Isaac eram responsáveis pelo treinamento e qualificação dos profissionais de inspeção anticorrosiva da ABRACO, e a Lúcia estava no Brasil para ministrar uma "conversa plenária" sobre a "Aplicação dos Princípios Enxutos na Proteção Contra Corrosão", como convidada do INTERCORR.

Como todos sabem, a ABRACO é a associação brasileira que representa os profissionais de corrosão no Brasil há mais de 50 anos, promovendo e disseminando o conhecimento sobre corrosão e proteção contra corrosão e qualificando profissionais em aplicação de tintas industriais, inspeção de pintura industrial, proteção catódica e inspeção de galvanização por imersão a quente. Além do exposto, a ABRACO também ministra cursos nas áreas de proteção anticorrosiva em equipamentos e dutos e proteção catódica em estruturas de concreto e de aço para os profissionais que desejam ampliar seus conhecimentos. O ICorr é o Instituto de Corrosão do Reino Unido, ou seja uma organização equivalente à ABRACO. Uma organização sem fins lucrativos cujos objetivos são o de disseminar os mais atualizados conhecimentos e técnicas usados na pesquisa e na prevenção da corrosão, assim como desenvolver as habilidades e qualificações em proteção anticorrosiva relevantes aos vários setores da indústria, principalmente nas áreas de proteção catódica e inspeção e aplicação de revestimentos anticorrosivos.

Após as apresentações, nós (Lúcia, Isaac e Flor) começamos a discutir os cursos profissionais de proteção contra corrosão de ambas as nossas organizações (ICorr e ABRACO), e identificamos uma grande sinergia entre nossos cursos e com isso, a possibilidade de uma cooperação mais estreita entre as organizações tornou-se o nosso alvo principal. Na sede da ABRACO no Rio de Janeiro, nós três fizemos uma apresentação ao então Presidente da ABRACO, Prof. Laerce de Paula Nunes. O objetivo da apresentação foi propor uma parceria que permitisse a divulgação do ICorr no Brasil, bem como a promoção da ABRACO internacionalmente. Além disso, queríamos obter um acordo e reconhecimento

1. ICATS – Treinamento para aplicadores de pintura industrial da Inglaterra

do ICorr para os inspetores de pintura treinados e qualificados no Brasil. Assim, proporcionaríamos aos inspetores de pintura da ABRACO uma qualificação reconhecida internacionalmente.

O projeto de colaboração "ICorr-ABRACO" foi imediatamente bem recebido pelo Presidente da ABRACO que, sob a orientação de Lúcia Fullalove, enviou mensagem à então Presidente do ICorr, Sarah Vasey, apresentando a ABRACO e explicando a intenção de criar uma parceria entre as duas organizações. A resposta do ICorr foi rápida e positiva, e "nós" começamos a delinear o projeto de cooperação em maio de 2018.

Inicialmente, parecia que a melhor maneira de progredir seria com uma comparação direta entre as qualificações de ambas as organizações nas áreas de inspeção de pintura, aplicação de tinta e proteção catódica. Assim, foi criado um Memorando de Entendimento (MoU) entre ABRACO e ICorr para delinear as intenções, os termos pactuados e, finalmente, o MoU foi assinado em junho de 2020 pelos então presidentes das duas organizações, Dra. Olga Ferraz (ABRACO) e Dr. Gareth Hinds (ICorr).

Essa parceria entre ICorr e ABRACO foi prevista para ir além do reconhecimento técnico, mas também permitindo maior exposição e reconhecimento do ICorr no Brasil, onde há um enorme potencial de desenvolvimento e treinamento devido ao tamanho do país e ao reconhecimento por grandes *players* em vários setores de mercado, em que a proteção contra corrosão é primordial e de grande benefício para os proprietários de ativos.

Por outro lado, a ABRACO é bastante reconhecida no Brasil pelo alto padrão de qualificação e qualidade da formação dos profissionais de corrosão, portanto a parceria com o ICorr manterá esses altos padrões e dará aos profissionais brasileiros a oportunidade de também contar com reconhecimento internacional.

Assim que o MoU foi assinado, nós (Isaac, Flor e Lúcia) começamos a trabalhar intensamente para focar na equivalência para a certificação de inspetores de pintura industrial. Desde o início, foi identificada a diferença entre os níveis de qualificação. No Brasil, a certificação dos inspetores de pintura é dividida em dois níveis, enquanto no Reino Unido é efetuada em três níveis. Portanto, o primeiro passo foi ver como a equivalência poderia ser alcançada e o caminho a seguir foi o de analisar e comparar os conteúdos programáticos dos cursos. A ideia era que esses fossem avaliados e decidida uma proposta de como essa equivalência poderia ser alcançada.

Em março de 2019, os conteúdos dos cursos de Inspetores de Pintura da ABRACO níveis 1 e 2 foram encaminhados para apreciação e avaliação pelo ICorr. John Fletcher (Gerente dos Cursos Técnicos de Revestimentos do ICorr) foi nomeado para realizar este trabalho e, em dezembro de 2019, após uma *Gap Analysis*, John identificou que o conteúdo do curso ABRACO Nível 1 abordava a maior parte do conteúdo dos cursos de Inspetores de pintura ICorr níveis 1 e 2, porém havia um déficit nas áreas de saúde e segurança do trabalho e, também, dos regulamentos da Organização Marítima Internacional (IMO) referentes a revestimentos de tanques de lastro. Na *Gap Analysis* inicial, John também propôs opções para a equivalência e um módulo de conversão.

Em março de 2020, no retorno ao Reino Unido, Lúcia fez uma apresentação ao ICorr PDTC (Comitê de Desenvolvimento e Treinamento Profissional do ICorr), durante a qual descreveu a empolgação e expectativa criada pelos inspetores de pintura brasileiros para essa "conversão" da certificação ABRACO para ICorr. Isaac, Flor e Lúcia produziram então um mapeamento entre os conteúdos programáticos e entre as Normas Brasileiras e Internacionais, para que o ICorr pudesse conhecer as Normas Brasileiras e entender que os inspetores de pintura brasileiros, apesar de trabalharem dentro das normas locais, possuíam um nível profissional de trabalho equivalente aos seus homólogos internacionais.

As demais diferenças foram identificadas em relação à legislação brasileira. Ao contrário do Reino Unido, no Brasil, as atividades

relacionadas à segurança e saúde ocupacional dos trabalhadores, em geral, são realizadas por um profissional da área de Saúde e por um engenheiro qualificado em Segurança do Trabalho. Além disso, as normas técnicas brasileiras são amparadas em lei, portanto, algumas das atividades de um profissional de proteção anticorrosiva devem ser seguidas em conformidade com a legislação. No Brasil, a norma determina até como os recipientes de tinta são empilhados no armazenamento.

Em 2022, sob a presidência e com o apoio da Dra. Zehbour Panossian conseguimos concretizar a primeira parte desse nosso objetivo com o lançamento do curso de Conversão.

O módulo de conversão bem como as questões do exame de conversão foram elaborados por Kevin Harold em nome do ICorr, o curso foi traduzido para o português, revisado e carregado no *IMechE Learning Management System* (LMS) e foi **lançado no Brasil em 28 de março de 2022**. Uma vez que o inspetor de pintura brasileiro faça o módulo de conversão e realize o exame de conversão on-line com sucesso, este obterá a sua certificação de inspetor de pintura ABRACO N1 validada como inspetor de pintura ICorr Nível 2.

Gostaríamos de ressaltar a nossa certeza quanto ao sucesso deste projeto. Esse foi um dos motivos pelos quais a Lúcia foi convidada a fazer uma apresentação sobre o projeto "ABRACO – ICorr" no Seminário Brasileiro de Pintura Anticorrosiva (SBPA) no Brasil em dezembro de 2019. Os principais participantes do evento foram inspetores de pintura e o projeto foi bem recebido pelo público.

Quando às atividades de treinamento e qualificação foram interrompidas como consequência da pandemia do COVID 19, Isaac, Flor e Lúcia intensificaram os trabalhos no curso de aplicadores de pintura industrial, estudando as possibilidade de como trazer o ICATS para o Brasil.

A ABRACO também queria ter o ICATS no Brasil na modalidade on-line e a Lúcia traduziu os módulos e vem trabalhando com Isaac para garantir o correto uso dos "jargões" locais e, também, a inclusão correta das práticas de trabalho brasileiras no curso. Os módulos ICATS traduzidos também foram carregados no sistema IMechE LMS para acesso on-line. Isso agora está sendo validado e, embora nenhuma data definitiva tenha sido acordada entre as partes para o lançamento do curso, um piloto deve começar em breve.

Assim como no Reino Unido, no Brasil o treinamento dos aplicadores de pintura industrial é feito em partes. A formação técnica de um Pintor Industrial do ICorr (ICATS) começa com um módulo sobre a compreensão dos princípios básicos de proteção contra corrosão, a importância de uma boa preparação de superfície (limpeza e tratamento) e o papel da tinta na proteção anticorrosiva. É nesse nível fundamental que o aplicador de pintura industrial será treinado no uso da trincha e do rolo. É intenção da ABRACO seguir essa sequência de treinamento que inclui pintura a pistola, jateamento abrasivo e hidrojateamento.

Em 2020, este projeto também foi apresentado ao Kevin Harold (Chefe Executivo da Correx

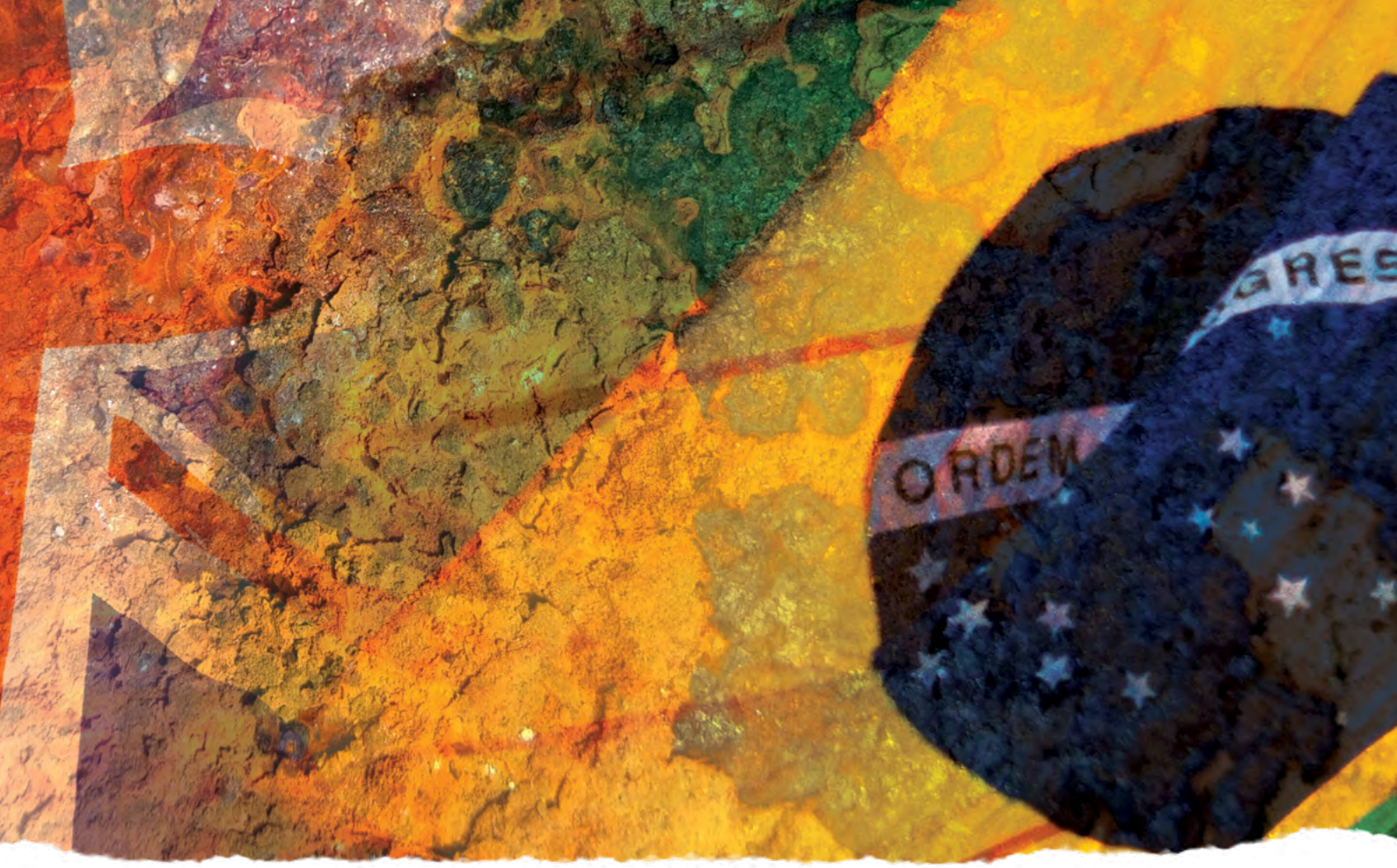

– Companhia do ICorr criada para ministrar o ICATS) que ficou entusiasmado com a perspectiva e propôs a criação do curso on-line de Aplicadores de Pintura Industrial (ICATS) em português para fornecer treinamento para pintores industriais no Brasil. As aulas práticas do curso bem como a avaliação técnica dos alunos (candidatos) serão feitas pela ABRACO.

O curso inicial (trincha e rolo) foi traduzido para o português e o seu conteúdo adaptado às exigências legais brasileiras, tanto em relação saúde, segurança e meio ambiente como aos procedimentos de trabalho.

Para a avaliação prática, Flor e Isaac já haviam desenvolvido um formulário para avaliar os alunos e que abrange todas as atividades realizadas por um pintor industrial. Isso foi compartilhado com Kevin Harold para ser avaliado e uma versão modificada foi produzida a qual será discutida para ser então aprovada em conjunto (Kevin, Isaac e Lúcia) como o novo formulário de avaliação para os Aplicadores Brasileiros de Pintura Industrial (ICATS – Brasil).

Em dezembro de 2020, ocorreu mais uma reunião virtual do Seminário Brasileiro de Proteção Anticorrosiva (SBPA), que contou com 130 participantes, para o qual o atual Presidente do ICorr, Dr. William (Bill) Hedges, e Kevin Harold também foram convidados. O Bill Hedges falou de sua alegria e confiança no sucesso desta parceria com a ABRACO, enquanto o Kevin Harold falou sobre o ICATS - Brasil e de seu entusiasmo pelo desenvolvimento do projeto com a ABRACO. A Lúcia fez uma apresentação sobre o progresso da cooperação entre ICorr e ABRACO. Na ocasião, houve novamente uma grande demonstração de interesse tanto dos inspetores de pintura quanto de pintores industriais esperando para poder fazer o curso de aplicador de pintura industrial - ICATS.

A parceria ICorr – ABRACO já é reconhecida e aguardada por diversos setores da indústria brasileira como petróleo e gás, siderurgia, mineração, petroquímica, fabricantes de tintas anticorrosivas entre outros. Existem ainda outras áreas de crescimento no Brasil onde temos certeza de que a força desta parceria será bem recebida.

Microencapsulation of methylmethacrylate to reinforced concrete addition for achieving self-healing and anticorrosive properties

Valério, D.[a], Aoki, I. V.[b]

[a] Civil Engineer – Master student at Polytechnic School of UNIVERSITY OF SÃO PAULO
[b] Chemist- Associate Professor at Polytechnic School of UNIVERSITY OF SÃO PAULO

Abstract

Reinforced concrete is one of the mostly used worldwide construction techniques. Nevertheless, pathologies as cracks and corrosion can reduce the lifetime of these structures and endanger users' lives. The objective of this research is to develop a self-healing system for concrete with anticorrosive properties. To achieve this goal, microcapsules containing an acrylic resin as a self-repair agent were developed to be doped in concrete. This way, when cracks start in the cementitious matrix, the healing agent is released from microcapsules, sealing cracks, and blocking aggressive agents' entrance. The characterization of microcapsules was performed by optical and scanning electron microscopy. To evaluate self-healing and anticorrosive properties, specimens of conventional and doped reinforced concrete were subjected to flexure tests according to ASTM C78 and electrochemical-technique analysis as polarization resistance (Rp) and electrochemical impedance spectroscopy (EIS). The results showed that the obtained microcapsules have appropriate morphology and size to be used in concrete. Moreover, flexural, EIS and *Rp* tests showed promising results for specimens doped with the proposed self-repair system.

Keywords: corrosion, concrete, self-healing.

Introduction

Concrete is one of the mostly used materials on the planet due to its easy molding in liquid state, good compressive strength, high availability of raw materials and low cost. As indicated by Pedroso [1], in accordance with Federacion Iberoamericana de Hormigon Premesclado (FIHP), 11 billion tons of concrete are annually consumed in the world, and it represents an annual average consumption of 1.9 tons of concrete per a land dweller.

One of the most common problems of reinforced concrete (RC) is the occurrence of fissures and cracks. According to Silva et al. [2], fissures can appear in RC due to many reasons, such as low tensile strength and/or occurrence of shrinkage in concrete. Albeit unwanted, the crack appearance is a natural phenomenon in RC structures, and its control is necessary to ensure structural integrity and durability of buildings. Fissures and cracks may work as an entrance preferential channels of aggressive agents which can cause corrosion of the steel reinforcement [2].

Corrosion matters with equipment and structures made of metal are quite common since this process occurs spontaneously and drives to degradation of them [3]. Despite being surrounded by concrete, carbon steel used as reinforcement in RC structures also corrodes. The agents that most commonly cause corrosion of RC reinforcement are chloride ions and carbon dioxide [4].

To make RC structures more durable and to reduce maintenance costs, the improvement of the concrete properties is necessary to make it less dependent on external repair interventions. One way to achieve this goal is to make concrete able to repair itself after cracks appear. Concrete with self-repair properties is called self-healing concrete (SHC).

There are some ways for concrete to have self-repair properties. One of them is to dope fresh concrete with encapsulated self-healing agents. In this way, when concrete becomes cured (hard), microcapsules act as reservoirs of a curing agent that is used on demand. In this case, when a crack appears in concrete, the microcapsules are broken, the curing agent is released and acts sealing the cracks [5].

In this work, the self-repair properties in concrete were obtained through the incorporation of a monomer and its polymerization activator in the concrete matrix in a fresh state. The monomer will previously be encapsulated in polymeric microcapsules while the polymerization activator will directly be added to the composite matrix.

Methodology

Production of microcapsules

The following chemicals were used as received to synthesize the microcapsules of poly-ureia-formaldehyde-melamine (PUFM) as shell containing methyl methacrylate (MMA) doped with N, N-dimethyl-p-toluidine (DMPT) as core: ureia, resorcine, arabic gum, sodium chloride, ammonium chloride, formaldehyde, and hydrochloric acid. All utilized chemicals were of analytical-purity degree.

The applied technique for producing the microcapsules was the emulsion polymerization. The method used for this is reported in the patent WO2014/032130 A1 [6]. The first step of the synthesis process was to produce an oil/water emulsion comprised of an aqueous solution of ureia, resorcine, arabic gum, sodium chloride, ammonium chloride and melamine as a continuous phase, and a solution of MMA and DMPT 1 % mass fraction as an oil phase. These two parts were vigorously mixed using a mechanical agitator for 30 minutes under an agitation rate high enough to ensure an appropriate size distribution of microcapsules. In the sequence, the formaldehyde was added to the emulsion, agitation rate and temperature were set for suitable values, and polymerization took place for several hours. After this process, the microcapsules were submitted to vacuum filtration, cleaned with acetone to remove non-encapsulated MMA solution, and left to dry at room temperature.

Reinforced concrete specimens' production

For preparing the RC specimens, ribbed rebars of carbon steel CA 50 with 6.3 mm diameter purchased from Gerdau, rebars of stainless steel 316 L with 6.3 mm diameter purchased from Maxfer, cement CP II F 32 MPa purchased from Votorantim, stone gravel with 19 mm maximum diameter, sand with 0.6 mm maximum diameter, tap water and benzoyl peroxide (BPO) were used.

Before beginning RC specimens' production, stainless steel and carbon steel rebars were cut in pieces of 35 cm length. Carbon steel rebars were carefully painted with an epoxy paint to limit the evaluation area in electrochemical tests, as can be seen in the Figure 1. RC samples were produced in a prismatic format with dimensions of 10 cm x 10 cm x 35 cm. In each specimen, one stainless steel and two ribbed carbon steel rebars were used. Concrete cover of 2.5 cm was used in every dimension that surrounded carbon steel rebars. All metallic rebars in RC specimens were carefully placed to ensure that 2.5 cm of each rebar was kept out of the specimen to be contacted. These rebars parts were used as an electric contact for electrochemical tests. Figure 2 shows in detail a reinforced concrete sample arrangement. The exposed areas for evaluation of carbon steel and stainless steel rebars were 39.6 cm^2 and 61.5 cm^2, respectively. The rest of the rebar's area was coated with an epoxy paint.

For conducting flexural and electrochemical tests, two sets of samples were prepared. The first group was used as a reference and was not doped with microcapsules. To the second set of specimens, 7 % mass fraction of microcapsules in relation to cement and 2 % mass fraction of BPO in relation to microcapsules were added. For all RC specimens, the used composition was 393 kg/m^3 of cement, 786 kg/m^3 of sand, 1179 kg/m^3 of stone gravel and 236 kg/m^3 of water. After RC specimens being unmolded, they were cured for 28 days in a humidity chamber.

A total of twelve RC samples were produced. These specimens were separated into two groups. Groups A and B were composed of six RC specimens each, three doped, and three undoped with microcapsules and BPO. For evaluating self-healing and anticorrosive properties of the proposed self-healing system, groups A and B were submitted to two different test routines.

Group A passed for electrochemical tests to provide results related to samples in the intact condition. On the other hand, group B was subjected to flexural tests to generate cracks, so they were left for a self-healing action period of 48 hours, and then, they were submitted to electrochemical tests. In this way, the samples of group B provided results related to damaged and healed conditions.

This approach was necessary to avoid a possible influence of samples' contamination with 3.5 % mass fraction NaCl solution used in electrochemical tests.

Microcapsule characterization

Microcapsule characterization was made to investigate the encapsulation of MMA and DMPT solution into PUFM microcapsules and to morphologically evaluate the microcapsules' shell.

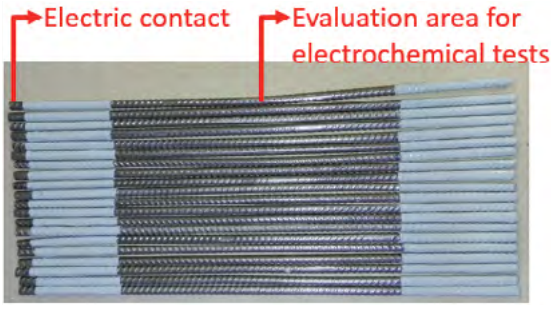

Figure 1 – Carbon steel rebars prepared to be used into RC specimen

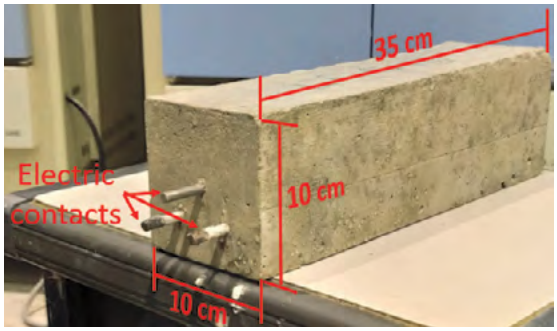

Figure 2 – RC specimen molded for electrochemical evaluations

For investigating the encapsulation, the Fourier transform infrared spectroscopy technique (FTIR) was used. On the other hand, the shell's morphology was evaluated through scanning electron microscopy (SEM).

FTIR analyses were carried out in three different substances. One in intact microcapsules, another in microcapsules that were previously broken, cleaned with acetone and air dried to remove all the MMA and DMPT solution and, finally, in the third substance composed only of the solution of MMA and DMPT. All FTIR analyses were made using a Bruker equipment model Alpha II FTIR -ATR spectrometer.

The micrographs obtained through SEM analyses were made using a Tescan equipment Vega 3 LM model.

Flexural tests

Flexural tests were conducted for causing cracks in the specimens stimulating the self-healing mechanism to act. The applied method was the four-point bending test, and it was carried out in accordance with ASTM C78 [7]. For this purpose, an INSTRON equipment model 8802 and a linear displacement sensor type LVDT were used. The rate and limit deformations used for performing the tests were 0.2 mm/min and 0.08 mm, respectively.

The samples were placed in the equipment with the longitudinal face which contains the carbon steel rebars facing down, and the equipment supports were positioned at 2.5 cm from the samples' vertical faces. Figure 3 shows the apparatus set up ready to perform the tests.

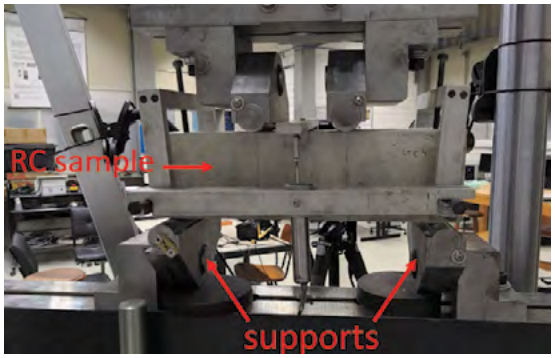

Figure 3 - Set up of the equipment used for four-point bending tests

Electrochemical tests

For investigating anticorrosive and self-healing properties, electrochemical impedance spectroscopy (EIS) and linear polarization resistance (Rp) tests were performed. The tests were carried out using an electrochemical arrangement with two electrodes. The working electrode (WE) was a carbon steel rebar whereas the counter electrode (CE) was a stainless steel one. Inputs of the potentiostat relatives to CE and reference electrode (RE) were short-circuited and connected to the stainless-steel rebar, as shown in Figure 5. The measurements were performed in the 3.5 % mass fraction NaCl solution, where the samples were partially immersed.

The tests were performed using a Gamry Instrument potentiostat, model Reference 600 controlled by the software Gamry Framework. All measurements were taken in the open circuit potential. The used parameters for EIS tests were potential amplitude disturbance of 10 mV rms, frequency range between 10^5 Hz and 10^{-2} Hz and 10 measurements per logarithmic decade. For Rp measurements, the parameters were potential disturbance of ± 10 mV around the open circuit potential, and a scan rate of 0.17 mV/s. The immersion times were 6 h, 24 h, 48 h and 72 h for both tests. Figure 4 shows the electrochemical cell used for EIS and Rp tests inside

Figure 4 - Set up of electrochemical cell used for EIS and Rp tests

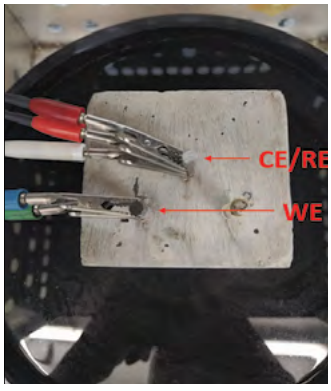

Figure 5 - Electrochemical arrangement used for EIS and Rp tests in detail

a Faraday cage, and Figure 5 shows the electrochemical arrangement in detail.

Results and discussion

Morphological characterization of microcapsules

The microcapsules composed of a shell of PUFM and a solution of MMA and DMPT as the core was characterized by SEM analyses. Figures 6 and Figure 7 show an overview and a high magnification of a representative microcapsules sample, respectively.

It is possible to observe in Figure 6 and Figure 7 that the microcapsules presented a well-defined spherical shape with a size distribution between 80 µm and 120 µm. Moreover, it can be noted that there is no microcapsules agglomeration tendency which is interesting because it facilitates its dispersion in the cementitious matrix.

Microcapsules characterization by FTIR

The encapsulation of the MMA and DMPT solution was investigated by FTIR technique, and the results are exposed in Table 1 and in Figure 8.

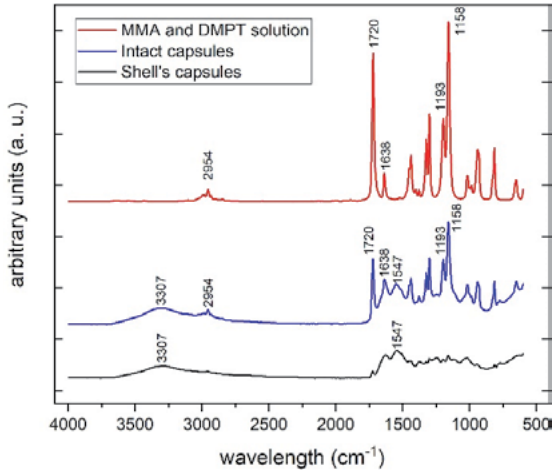

Figure 8 - FTIR spectra obtained for MMA and DMPT solution, for intact capsules and for empty capsules

Table 1 shows the main peaks, their wavelength positions, and their attribution to functional groups which could be identified in the analyzed substances. The table's first column exposes the wavelength positions used as references for results discussion according to [8–11].

Analyzing the spectrum obtained for the MMA and DMPT solution, some bands were able to be observed. The first in 2964 cm^{-1}, which can be attributed to a C–H stretch, is related to

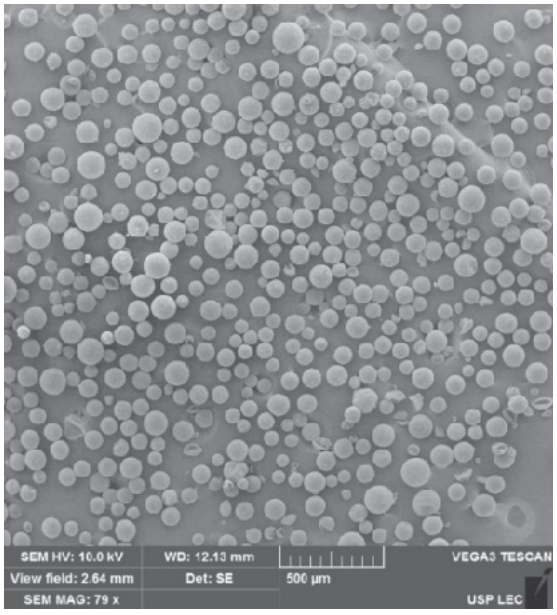

Figure 6 – SEM overview of microcapsules containing MMA and DMPT

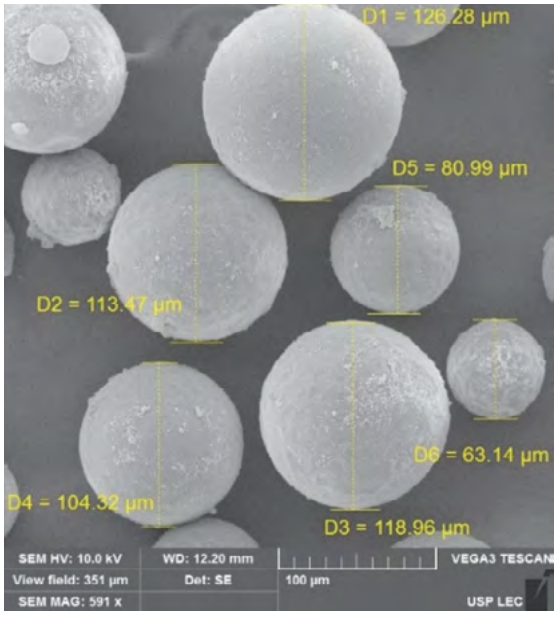

Figure 7 – SEM high magnification of microcapsules containing MMA and DMPT

Table 1 – Attribution of main peaks identified in the FTIR spectra in Figure 8

Chemical bonds/reference wavelength values (cm^{-1})	Wavelength obtained from FTIR spectra (cm^{-1})		
	MMA + DMPT (1 % mass fraction)	Intact microcapsules	Microcapsules' shells
N – H stretch/3150 - 3600	Absent	3307	3307
N – H angular deformation / 1548	Absent	1547	1547
C–H stretch / 2872 – 2962	2954	2954	Absent
C=O stretch / 1740 – 1715	1720	1720	Absent
C=C stretch / 1640 - 1625	1638	1638	Absent
C–O stretch / 1300 – 1000	1193 and 1158	1193 and 1158	Absent

alkyl and methoxy groups of MMA [8]. Other two bands, with wavelengths of 1720 cm^{-1} and 1638 cm^{-1}, were also observed and are related to the C=O and C=C stretching which are present in the MMA monomer. Furthermore, two bands with wavelengths of 1193 cm^{-1} and 1158 cm^{-1} were observed and are related to the C–O stretch in MMA [9,10].

In the microcapsules' shell spectrum, one band and one peak were able to be seen, the band with the wavelength of 3307 cm^{-1} and the peak with wavelength in 1547 cm^{-1}. According to Gomes [8], Silverstein *et al.* [10] and Yuan Li et al. [11], the band in 3307 cm^{-1} is related to symmetrical and asymmetric stretches of N–H that occurs in the same region, whereas the peak in 1547 cm^{-1} is related to angular deformation of the same chemical bond, both belonged to polyurea. These two bands were also identified in the intact microcapsules spectrum and were not verified in the MMA and DMPT solution. It shows that these specific bands are related to the shell's microcapsules. In the intact microcapsules and microcapsules' shell spectra, a band in 1638 cm^{-1} was observed. This band is related to the amide carbonyl group which is absorbed in a lower frequency due to a resonance effect [8].

Finally, observing the spectrum of intact microcapsules, the presence of bands with wavelengths at 2954 cm^{-1}, 1720 cm^{-1}, 1638 cm^{-1}, 1193 cm^{-1} e 1158 cm^{-1}, which are characteristics of chemical bonds related to the monomer, were able to be verified. In addition, bands with wavelength of 3307 cm^{-1}, 1638 cm^{-1} and 1547 cm^{-1} that are related to functional groups, which belong to shell's microcapsules, were able to be observed. It proves that the healing agent was successfully encapsulated in PUFM shells.

Evaluations of self-healing effect and anticorrosive properties by electrochemical tests

The electrochemical tests were performed under four different conditions that were divided and codified to make the comprehension easier. The first condition is related to samples with no capsules and no cracks. They were called as positive references (POS_REF). The second condition is related to specimens with no capsules but with cracks. They were codified as negative references (NEG_REF). The third condition was related to samples with capsules but no cracks. They were codified as ADT_WNC. Finally, the fourth condition was related to samples with capsules and with cracks. They were codified as ADT_WC.

EIS tests

Results of EIS measurements were plotted in Bode and Nyquist diagrams. Figures from 9 to 12 show the results obtained for all evaluated conditions.

In the impedance measurements for reinforced concrete, the response observed at high frequencies (HF) is related to the electrolyte which, in this case, is the concrete and the NaCl solution capable of percolating through the specimen [12,13]. On the other hand, at

low frequencies (LF), it is possible to observe the response of carbon steel used as a working electrode in electrochemical tests, making it possible to identify the occurrence of corrosion or the passivity of the steel reinforcement. It is important to point out that in this paper, the immersion periods were not long enough to allow significative changes in |Z| at LF. Based on this, in Bode diagrams, the values of |Z| in HF (105 Hz) were mainly analyzed. It was made to evaluate the response of RC samples and relate it with concrete's percolation resistance. Andrade et al. [14] and Wu et al. [15] claim that there is a direct proportional relationship between a concrete's resistivity and the rate of corrosion of metallic rebars embedded in the concrete. Thus, the higher this value, the lower NaCl solution percolation through cementitious matrix, therefore, the corrosion of the steel reinforcement will most likely be less.

For analyzing Nyquist diagrams, a special attention was given for Z_{real} values at frequency of 5.0 kHz. It was made because, in this frequency, an intersection of the two semicircles (characteristic of Nyquist plots for reinforced concrete) occurred. This intersection is important in the analyses because this point can be related to the percolation resistance of concrete [13,15].

In Figure 9C (Nyquist diagrams), it can be observed that for the immersion time of 6 h, samples of positive reference presented Z_{real} of 3200 Ω.cm² at 5.0 kHz. After 24 h of immersion, there was a sudden fall in this value, followed by a stabilization in a value next to 2300 Ω.cm². The same behavior was observed in the Bode diagrams |Z| modulus x frequency shown in in Figure 9A in which the |Z| values in HF (attributed to the concrete resistance) presented the same fall. The decrease of Z_{real} at f = 5.0 kHz and |Z| in HF values can be explained by the hindered permeation of the saline solution in RC samples since this can cause a decrease in the concrete resistivity. However, corrosion of carbon steel reinforcement was not verified because there were not new time constants during the test period as seen in Figure 9B.

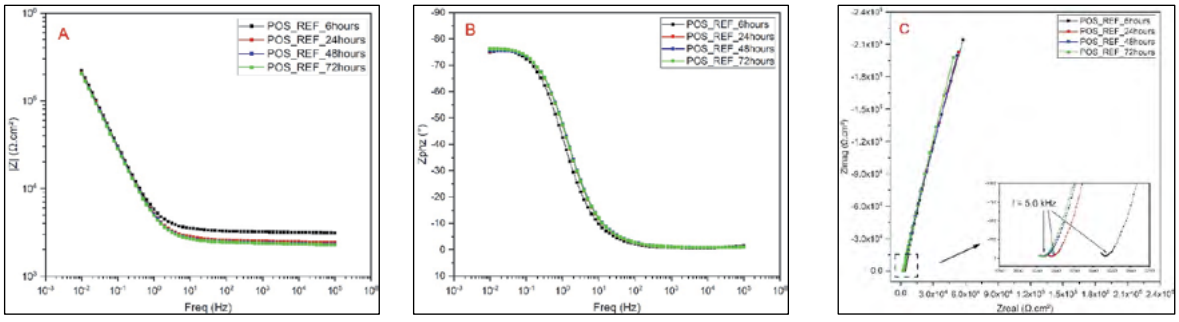

Figure 9 - EIS results for positive reference samples immersed in 3.5 % mass fraction NaCl solution. A) Bode plot of |Z| x Freq. B) Bode plot of (°) x Freq. C) Nyquist.

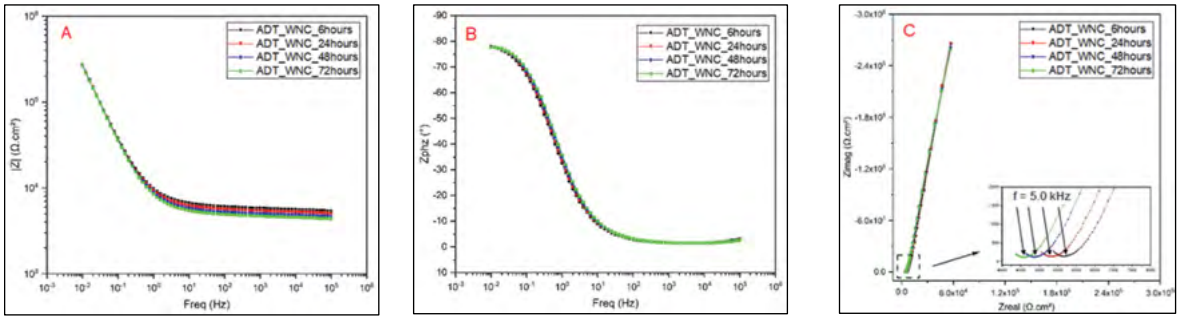

Figure 10 - EIS results for samples with additivation and with no cracks immersed in 3.5 % mass fraction NaCl. A) Bode plot of |Z| x Freq. B) Bode plot of (°) x Freq. C) Nyquist.

Analyzing the results obtained for ADT_WNC samples, Figure 10, a behavior slightly different of those presented by positive references was able to be noted. The first difference was the concrete's resistivity falling. This was caused by the percolation of the saline solution in the cementitious matrix. This percolation occurred in a slower way as Z_{real} at f = 5.0 kHz and |Z| in HF did not present abrupt falls. Instead of this, a soft drop was observed as seen in Figure 10A.

Another important point to be mentioned was the fact that Z_{real} at f = 5.0 kHz and |Z| in HF values were approximately 5600 Ω.cm² for the immersion time of 6 h and 4600 Ω.cm² for 72 h. Comparing these values with those of positive reference, it was noted that the addition of self--healing system hindered the percolation of the saline solution through the concrete.

Evaluating the results obtained for samples with cracks, NEG_REF and ADT_WC, a similar behavior of that of POS_REF was observed. In Figure 11, it was noted that NEG_REF samples presented Z_{real} at f = 5.0 kHz and |Z| in HF values after 6 h of immersion of approximately 3300 Ω.cm². This value dropped abruptly to the plateau of 2200 Ω.cm² which was kept for the following hours. On the other hand, in Figure 12, it is observed that ADT_WC samples exhibited values of Z_{real} at f = 5.0 kHz and |Z| in HF of approximately 3700 Ω.cm² for the immersion period of 6 h, followed by a decrease down to 3050 Ω.cm² for the immersion time of 24 h. In the next hours, a stabilization in 2850 Ω.cm² was verified. Here, it was possible to observe that doped samples presented higher values of the concrete resistance to electrolyte permeation for whole of the immersion period, showing that the addition of concrete with the proposed self-repair system hindered the percolation of NaCl solution and consequently decreased the probability of steel reinforcement corrosion.

For summarizing the EIS results, Figure 13 exposes the diagram of the Z_{real} at f = 5.0 kHz average values x immersion time.

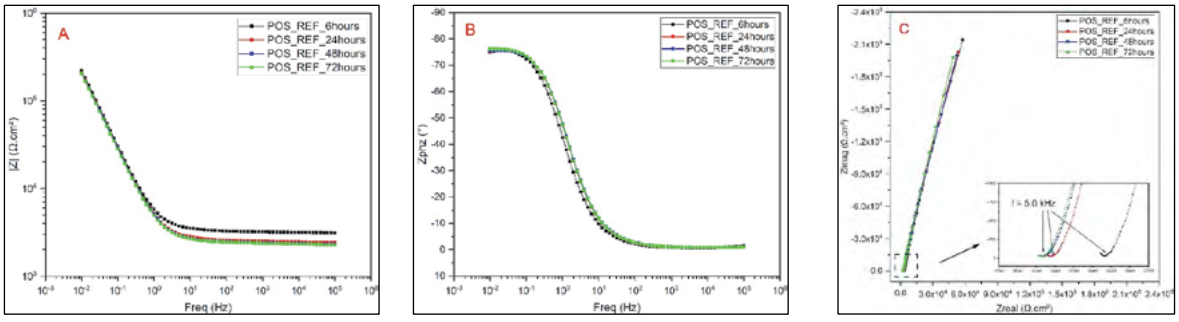

Figure 11 - EIS results for samples with no additivation and with cracks immersed in 3.5 % mass fraction NaCl solution. A) Bode plot of |Z| x Freq. B) Bode plot of (°) x Freq. C) Nyquist plot.

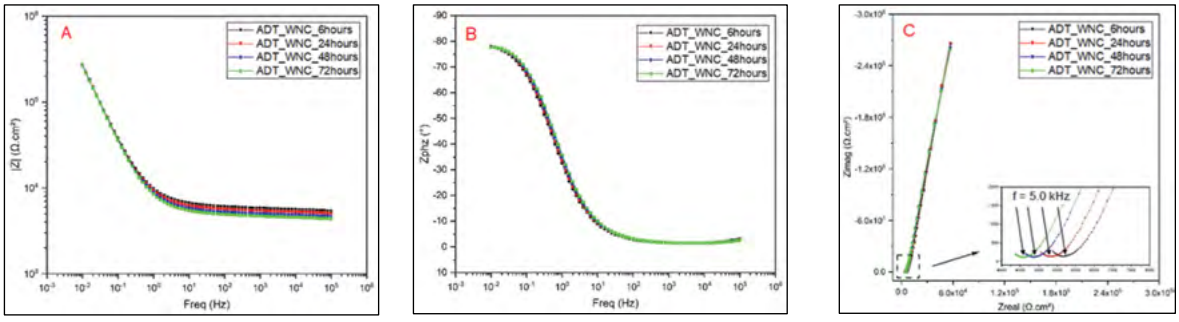

Figure 12 - EIS results for samples with additivation and cracks immersed in 3.5 % mass fraction. A) Bode plot of |Z| x Freq. B) Bode plot of (°) x Freq. C) Nyquist plot.

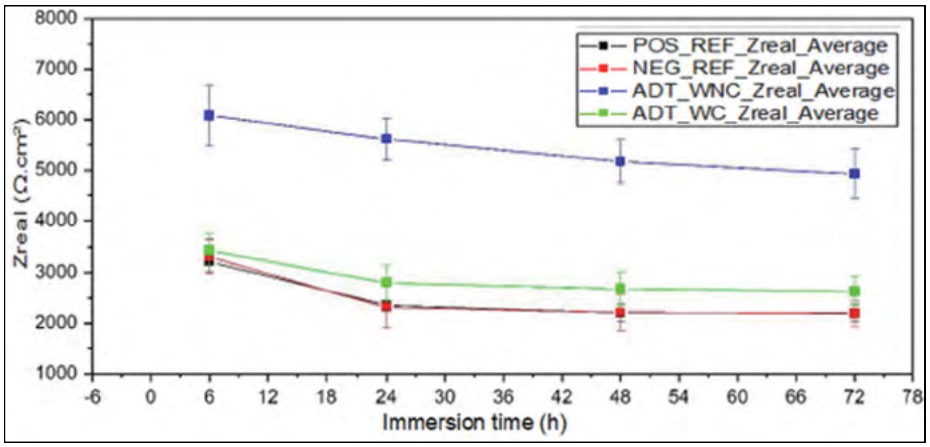

Figure 13- Average concrete resistance (Zreal at f = 5.0 kHz) values x immersion time plot, for all evaluated conditions

The analysis of Figure 13 clarifies the downward trend of the concrete resistivity in the evaluated conditions due to the percolation of the NaCl solution. As previously discussed, the drop in the resistance of the reference specimens with and with no cracks, NEG_REF and POS_REF respectively, was high during the first 6 h of immersion and these values tended to be stabilized in the following hours. Furthermore, it could be noted that the doped and cracked sample resistance, ADT_WC, despite being statistically equal to those of POS_REF and NEG_REF conditions, exhibited a less pronounced downward tendency. In addition, it could be observed that the ADT_WNC sample condition showed absolute values of Z_{real} bigger than the samples of the other conditions, revealing that the additive increased the concrete resistance to the NaCl solution percolation.

Rp tests

In order to treat the data in such a way that the results could point out the electrochemical behavior of the specimens, a smaller set of data from Rp curves of each condition was selected. It was made to ensure that the selected data could be compared to a straight line, allowing the calculus of i_{corr}. In this way, points of the Rp curves were selected to the right and left of the zero current until it was possible to draw a linear trend line which touched tangentially the selected data sets, with R^2 above 0.95. Once the trend lines were drawn, the slopes of the lines that are the Rp values of each straight line were found. With the Rp values, the Stern and Geary equation was applied to obtain the icorr values for each analyzed curve. With the i_{corr} values, i_{corr} x time plots were drawn up with the average values of the triplicates of each group. The final graphic is shown in Figure 14.

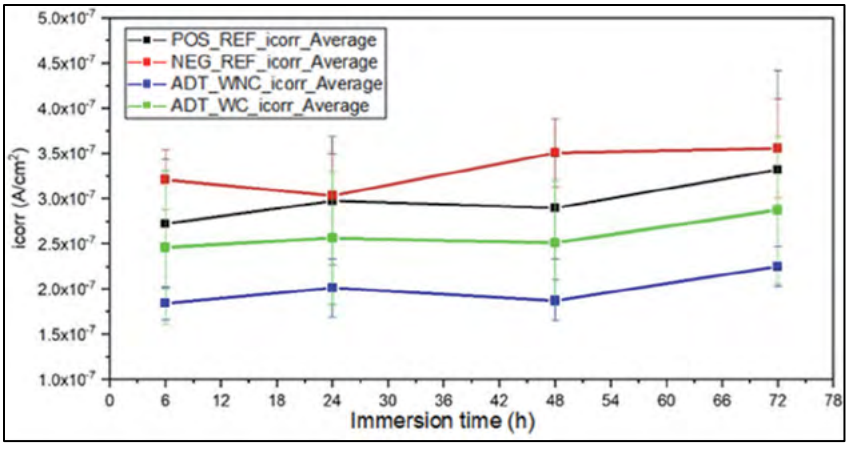

Figure 14 - Diagram of average i_{corr} values x immersion time for all evaluated conditions

The analysis of Figure 14 shows that the i_{corr} values have a slight upward trend for all evaluated systems during the studied period.

However, despite there being a certain variation as can be seen in the error bars, the absolute values show, as did EIS test results, that the ADT_WNC system was the one that best performed electrochemically since the i_{corr} values of this system were the smallest, showing lower corrosion rates compared to the positive and negative references. The error bars indicate a large standard deviation for the triplicate samples which makes a fair comparison between groups difficult. Despite this, it was possible to verify that the addition of microcapsules in the concrete provided greater resistance against the percolation of the NaCl solution, pointing out the potential capacity of the additive to decrease the ingress of the aggressive agent chloride ions, of water and oxygen.

Conclusions

The results of FTIR analysis and scanning electron microscopy showed that the mixture of MMA with DMPT was successfully trapped in the polyurea-formaldehyde-melamine shell and that the microcapsules had a spherical shape and size distribution between 80 μm and 120 μm. Moreover, the electrochemical tests showed an increase in the resistance of the concrete against the percolation of the NaCl solution which resulted in a decrease in the corrosion rate of the doped systems in relation to the non-doped ones. Such results accredited the proposed system for being deeply studied.

References

[1] PEDROSO, F. L. Concreto: as origens e a evolução do material construtivo mais usado pelo homem. **Revista Concreto & Construções - Instituto Brasileiro de Concreto (IBRACON)**, v. XXXVII, n. 53, p. 77, 2009.

[2] SILVA, R. C. **Vigas De Concreto Armado com telas soldadas : Análise aeórica e experimental da Resistência à força cortante e do controle da fissuração.** São Carlos. Universidade de São Paulo, 2003.

[3] GENTIL, V. **Corrosão**. 3. ed. Rio de Janeiro: LTC - Livros Técnicos e Científicos, 2007.

[4] KUMAR, V. Protection of steel reinforcement for concrete - A review. **Corrosion Reviews**, v. 16, n. 4, p. 317–358, 1998.

[5] GILFORD, J.; HASSAN, M. M.; ASCE, M.; RUPNOW, T.; BARBATO, M.; OKEIL, A.; ASADI, S. Dicyclopentadiene and Sodium Silicate Microencapsulation for Self-Healing of Concrete. **Journal of Materials in Civil Engineering**, v. 26, n. 5, p. 886–896, 2014.

[6] AOKI, I. V.; SOLYMOSSY, V.; FERREIRA, P. A.; KOEBSH, A.; COELHO, J. F. P. **WO 2014/032130 AlBrasil**, 2014.

[7] MATERIALS, A.-A. S. FOR T. **Standard Test Method for Flexural Strength of Concrete (Using Simple Beam with Third-Point Loading)**, [s.d.].

[8] GOMES, S. R. **Revestimentos com propriedades de autorreparação contendo metacriloxipropiltrimetoxisilano como formador de filme**. São Paulo. Universidade de São Paulo (USP), 2019.

[9] PAVIA, D. L.; LAMPMAN, G. M.; KRIZ, G. S. **Introduction to spectroscopy : a guide for students of organic chemistry**. 3. ed. California: Fort Worth Harcourt College, 2001.

[10] SILVERSTEIN, R. M.; WEBSTER, F. X.; KIEMLE, D. J. **Spectrometric identification of organic compounds**. 7. ed. New York: Wiley, 2005.

[11] YUAN, L.; LIANG, G.; XIE, J. Q.; LI, L.; GUO, J. Preparation and characterization of poly(urea-formaldehyde) microcapsules filled with epoxy resins. **Polymer**, v. 47, n. 15, p. 5338–5349, 12 jul. 2006.

[12] DÍAZ, B.; GUITIÁN, B.; NÓVOA, X. R.; PÉREZ, M. C. The effect of long-term atmospheric aging and temperature on the electrochemical behaviour of steel rebars in mortar. **Corrosion Science**, v. 140, p. 143–150, 1 ago. 2018.

[13] RIBEIRO, D. V.; SALES, A.; SOUSA, C. A. C.; ALMEIDA, F. DO C. R.; CUNHA, M. P. T.; LOURENÇO, Z.; HELENE, P. **Corrosão em Estruturas de Concreto Armado: Teoria, controle e Métodos de Análise**. First ed. São Paulo: Campus, 2013.

[14] FELIU, S.; GONZÁLEZ, J. A.; FELIU, S.; ANDRADE, C. Relationship between conductivity of concrete and corrosion of reinforcing bars. **British Corrosion Journal**, v. 24, n. 3, p. 195–198, 20 jan. 1989.

[15] WU, L.; DAI, P.; LI, Y. Determination of the Transport Properties of Structural Concrete Using AC Impedance Spectroscopy Techniques. Journal of engeneering, v. 2, p. 8, 2016.

Issues with thermal insulation painting

Pedro R. P. Viana[a], Flávio V. V. de Souza[b], Thiago R. de Almeida[c], Victor H. D. M. Santos[c], Wang Liangzhuang[c], Oswaldo E. Barcia[d], Isabel C. P. Margarit-Mattos[e]

[a] Pós Doc, UFRJ / COPPE / PEMM / LNDC
[b] DSc, Researcher, UFRJ / COPPE / PEMM / LNDC
[c] IC, Undergraduate Students, UFRJ / POLI / DMM / LNDC
[d] DSc, Professor, UFRJ / IQ / DFQ / LNDC
[e] DSc, Professor, UFRJ / POLI and COPPE / PEMM / LNDC

Abstract

Thermal insulation paintings involve relatively new technology compared to conventional thermal insulators used in metallic structures exposed to the atmosphere. The objective of this work is to discuss aspects of this technology, presenting advantages and limitations that still need to be overcome to improve its industrial application. The adopted approach consists of a critical evaluation of the characteristics of commercial products recognized in the market, comparing information provided in their technical sheets, with respect to application criteria, thermal properties and corrosion protective properties. This assessment can also point out possibilities for the development of this technology. Some comments are corroborated by experimental results obtained in laboratory, which seek to disseminate and to elucidate mechanisms for the performance of these products, contributing to a culture of more grounded use of this relatively new coating technology.

Keywords: corrosion, coating, thermal insulation

Introduction

The unwanted transfer of thermal energy can generate problems in industrial processes, affecting the flow of fluids, phase stabilization, energy efficiency and personal protection. The solution to these problems demands the use of thermal insulators. Conventional thermal insulators consist of thick layers that make it difficult to detect CUI (corrosion under insulation) and to inspect the structural integrity of the equipment. In general, conventional insulators also involve difficulties in application and maintenance, especially in structures with complex geometries. As an alternative, there are thermal insulation paints that, in principle, can act with a few millimeters of thickness, facilitating inspection procedures. Another advantage is that they can be applied by usual methods of industrial painting, facilitating maintenance and providing advantages from an economic point of view. These products have been on the market for over ten years with very heterogeneous technical files. This makes it difficult for users to choose the most suitable product and the expectation of performance is based mainly on the credibility of the supplier. In this context, three important aspects for analysis are highlighted: i) there is no consensus on the methodology for characterizing the thermal properties of paints; ii) it is not known how the thermal properties of these paints vary according to the time and environmental conditions of service, that is, with their aging process, and iii) there is no consensus in the methodology for characterizing the anticorrosive properties of these paints. These aspects are disclosed in this work with a search for literature and information on technical datasheets for commercial thermal insulating paints. In this way, the state of the art of this type of product is evidenced, as well as a critical evaluation is made of some procedures mentioned in order to assist the development of technical specifications by large users, stimulating greater homogenization of information in the supplier files and contributing for a culture of more grounded use of this "new" coating technology.

Methodology

Five commercial thermal insulation paints from internationally recognized brands were selected. Each liquid paint was identified by letters from "A" to "E". This work involves: i) critical evaluation of the technical files; ii) brief comparison of some standards cited for measures of thermal properties; iii) discussion of experimental results related to corrosion protective properties. The experiments consisted of measures of water absorption and water vapor permeability of free paint films at 23 °C. These are important properties for corrosion protection and can also influence thermal properties during service. Carbon steel mass loss tests were also carried out on aqueous extracts of the paintings films obtained at 25 °C [1] for preliminary evaluation of the existence of substances in paints, leaching during electrolyte permeation, which can influence the corrosion rate of the base steel, accelerating or inhibiting this process. Viscoelastic properties of the paintings were characterized by DMA (dynamical mechanical analysis) complementing the experimental results.

Results and Discussion

Of the five paints evaluated, four were one-component paints with a water-based acrylic vehicle (A, B, C and D) and one was two-component epoxy, also water-based (E). The type of filler added with the thermal insulating function was only mentioned by one supplier. However, the description of the most frequent insulating filler in the literature is hollow ceramic microspheres (TiO_2, glass) and air gel silica [2-5].

DMA representative results for acrylic paints A-D are shown in Figure 1 (a) and, for the epoxy paint E, in Figure 1 (b), allowing to characterize the temperatures at which important transitions occur in the materials structure and verify which of them can affect its mechanical behavior among other properties. The three dotted lines were placed at 25 °C, 60 °C and 180 °C. At the operating limit temperature (180 °C) all paintings are in rubbery state.

This seems to be the conception in the formulation of thermal insulating paints which guarantees the lowest thermal conductivity of the polymeric matrix since the rubbery state is characterized by a greater free volume than the glassy state. As the temperature decreases to the safe touch limit (60 °C), the acrylic paints A-D remain in the rubbery state, while the epoxy paint E is already in a transition state close to the glassy state. The decrease in temperature restricts the mobility of the material. If moisture is absorbed and operating temperature variations are in the transition range of the coating, stresses can be generated because the absorbed water cannot be released timely. Relaxation of these stresses can result in loss of adhesion at the interfaces and/or crack nucleation, depending on the mechanical properties of the coating [6]. Swelling is also a possibility. Epoxy paints are more prone to loss of cohesion and acrylic paints are more prone to swelling. However, the content and nature of the fillers can greatly influence this behavior. Then, the characterization of thermal insulation paints should be complemented with measures of mechanical properties. At room temperature of 25 °C, the paints are at different transition levels. On the one hand, the rubbery state is suitable for thermal insulation, on the other hand, the anti-corrosion barrier properties are not good. In Figure 1, it can be seen that at 25 °C, E paint is the only one that is close to the vitreous state. This is the temperature at which several complementary laboratory tests were carried out. Therefore, it is necessary to consider this factor because the structure of the dry film of this paint is different in the three considered conditions. For example, E paint was the one with the lowest permeability and absorbed less water with slower kinetics, see Figure 2. However, at the temperature at which the absorption test was carried out (23 °C), the structure of the dry film of this paint is different from that at higher temperatures. The other paints do not experience structural transitions under these experimental conditions.

Figure 2 shows that the classification of paints in terms of water absorption (Figure 2 (a)) is the same as that made in terms of water vapor permeability (Figure 2 (b)), that is, the paints with the highest absorptions also are the most permeable. This characteristic is desirable because it does not favor water retention at the interface paint/metal, making CUI more difficult. On the other hand, if the insulating paint is applied over an anticorrosive primer, it is the behavior of the primer that will define the corrosion resistance of the system. This characteristic of high absorption and high permeability suggests poor barrier properties. What about the use of top coatings? It would be interesting to complement this information by monitoring the electrochemical impedance of

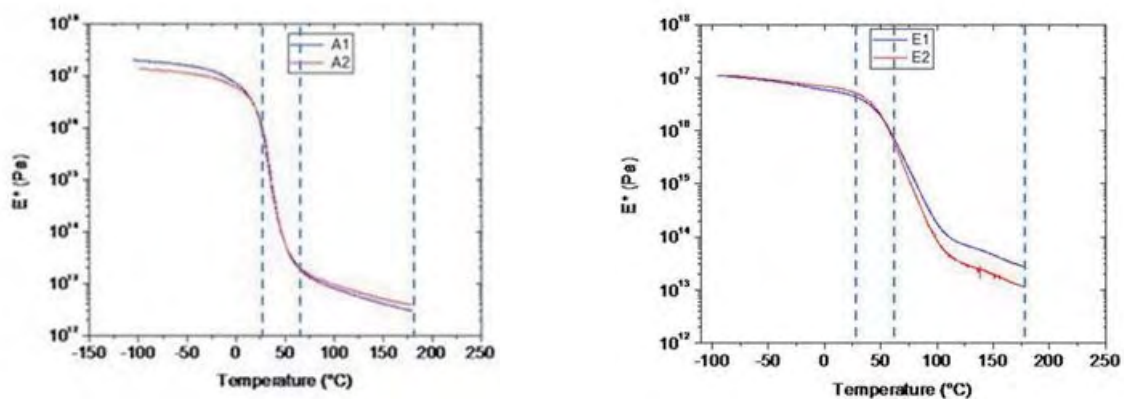

(a) **(b)**

Figure 1 - Complex module obtained from DMA measurements as a function of temperature. (a) Paint A representing the behavior of acrylic paints; (b) Epoxy paint E.

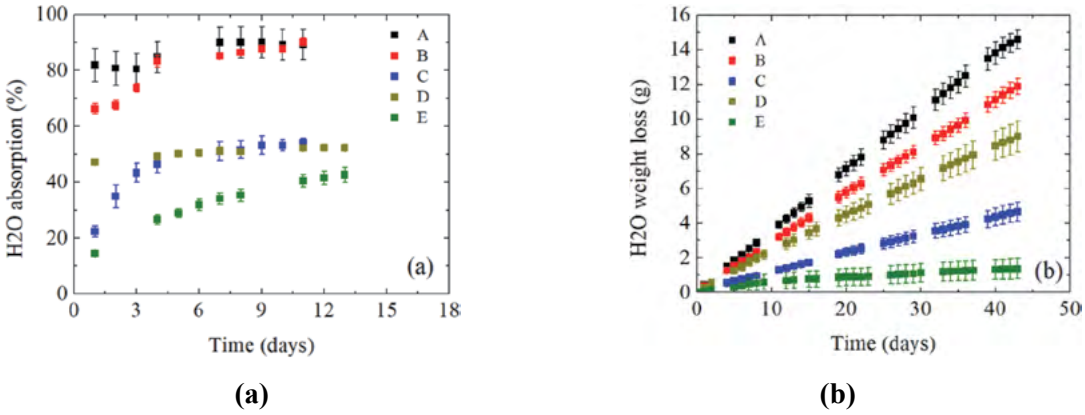

(a) **(b)**

Figure 2 - (a) Water absorption and (b) Water vapor permeability of thermal insulation paintings.

painted samples during corrosion tests. There is a consensus in the literature that impedances greater than 10^6 Ω.cm^2, in long-term tests, can be related to good barrier properties.

Some anticorrosive primers suggested in the technical data sheets of insulating paints are: phenolic epoxy, high pigmented epoxies with Al, mastic epoxy, moisture and surface tolerant epoxies, thermal variation tolerant composite coatings, many primers with Novolac vehicles, low VOC and high solids content, in addition to zinc-rich primers (ZRP). This last suggestion is questionable and needs to be carefully evaluated. It is known that metallic Zn presents an inversion of electrochemical potential in relation to carbon steel at high temperatures. In this case, the ZRPs would stimulate CUI by galvanic action in the presence of moisture. Its recognized cathodic protection mechanism would not operate under these conditions. Indeed, reports of failure in structures with ZRPs under thermal insulation can be found in the literature [7-8].

As general characteristics, epoxy paintings have greater hardness, resistance to abrasion and impact than acrylic paintings. They are known for their chemical resistance and their corrosion protection capacity. However, it is worth noting that epoxy paints, when exposed to natural weathering, have poor resistance to UV rays and, consequently, they lose brightness and color very quickly. In addition, they present chalking and blistering. Therefore, in the case of the epoxy-based thermal insulating paint applied to a structure exposed to solar radiation, this consideration in its formulation or the use of a UV-resistant topcoat is important.

In the formulation of water-soluble paints, to be used as a primer, it is advisable to have an inhibiting pigment to prevent flash-rust, the occurrence of which was verified in different degrees, during the application of all the products evaluated in this work. The worst case is shown in Figure 3.

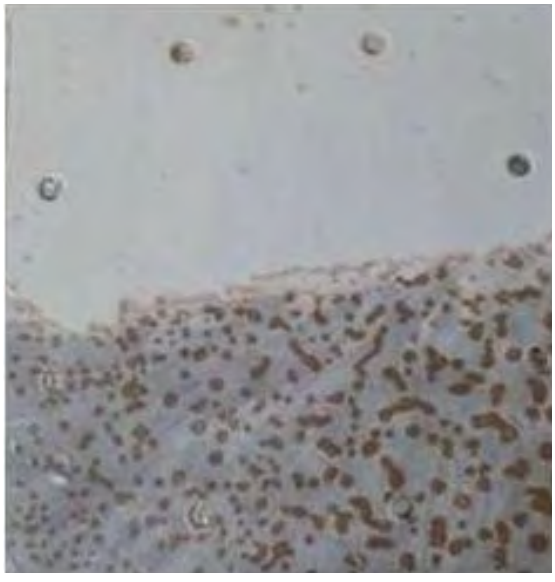

Figure 3 - Sample with partial removal of the dry paint film with corrosion of the base steel caused by the paint during application.

The verification of the presence of corrosion inhibitors in the insulating paints was done with mass loss testing of the steel in aqueous extracts of the painting films, obtained at 25 °C. After 14 days of testing, uniform corrosion was observed in all cases. The obtained corrosion rates are shown in Table 1 for triplicate samples. The solution called *Control* is water used to obtain the extracts. The measured corrosion rates in the extracts of the five paints were less than or equal to those of the control solution which shows that the leachable species at 25 °C do not stimulate the corrosion of the steel. In some cases, there is even a corrosion inhibiting effect. In this respect, C was the paint that showed the highest inhibition efficiency.

The occurrence of flash rust during the application may also justify the need for a primer. However, the characteristics of the anticorrosive primer need to be considered in order not to restrict the operating and application temperatures of insulating paints. This last factor is presented in several technical sheets as an advantage of insulating paints, that is, the ease of application on hot surfaces, without stopping the equipment for maintenance. If there is a primer in the painting system, it should also have the same features.

Table 1 - Corrosion rate of steel in aqueous extracts of the painting films obtained at 25 °C.

Solution	Corrosion rate (mm/year)
Control	0.06/ 0.06 / 0.06
Extract of A	0.05/ 0.04 / 0.04
Extract of B	0.04/ 0.04 / 0.04
Extract of C	0.02/ 0.02 / 0.02
Extract of D	0.06 / 0.06 / 0.05
Extract de E	0.05 / 0.05 / 0.04

In Table 2, the application conditions are summarized. In principle, there are arguments emphasizing the ease of application compared to conventional thermal insulation paints which are true. However, acrylic paints only allow for wet thicknesses of around 500 µm per coat; epoxy paint admits greater wet thickness. For personal protection, with the surface exposed to safe touch at 60 °C, and equipment operating at 180 °C, the dry thickness recommendations imply multi-coat: 4 to 9 coats for acrylic paints and a smaller number, 2 coats, for epoxy E paint. The average interval is 2 h between coats, depending on the relative humidity. Thus, the application of insulating paints may be simpler compared to conventional insulators and more convenient for complex geometries, but still, the demand for man-hours is high. A comparison of the application conditions of acrylic and epoxy thermal insulation paints has already been carried out by Baer [9].

Thermal insulation capacity depends not only on the polymeric matrix, but also on the fillers. As already reported, in most cases, they consist of hollow microspheres. Hence, the homogenization and application care recommended by the manufacturers must be strictly obeyed. The use of suitable nozzles and pressure regulation in the airless application should avoid the collapse of the fillers which will certainly impair the insulating effect of the film. Still, regarding the behavior of the fillers, it is considered important to check their integrity during long-term high-temperature expositions, due to the risk of microspheres collapsing and, also, with thermal shocks due to the fragility of the microsphere by thermal fatigue, especially if it is made of glass. In this context, corrosion tests involving temperature cycles can have a dual function: to characterize anticorrosive performance and to evaluate the resistance of fillers to temperature variations. This is an aging aspect that is very peculiar to thermal insulation paints: the possibility of deterioration of insulating fillers, compromising the thermal performance.

The indication of the need for a topcoat, either for mechanical resistance or to provide better barrier properties, is less frequent in technical sheets. This is another aspect that requires a complementary characterization of each product. As shown in Figure 2 (a), paints A and B have fast and high water absorption at a mild temperature of 23 °C. The increase in

temperature favors this process even more. The other paintings have slower absorption kinetics. C and D saturate with 50 % absorption. The painting with the lowest absorption is E. It is worth remembering that these results depend on the temperature. Based on the DMA measurements, the greatest variation for paint E is expected due to the important structural transitions in the temperature range 60°C to 180 °C.

The dimensioning of the thicknesses depends on the thermal properties of these paintings. As can be seen in Table 3, there is no homogeneity in the information provided by the manufacturers. In addition, there is no information about the variation of the paint characteristics with the painting aging process. Without a topcoat, moisture will be absorbed. Therefore, it is important to know the variation of thermal properties with the absorption of water for conservative dimensioning of thicknesses. Specifically considering the case of insulation for personal protection, thermal conductivity would be the most important property. To determine the thermal conductivity, the technical data sheets mention three standards: ASTM C335, ASTM C177 and ASTM C518.

The ASTM C335 standard, *Standard Test Method for Steady-State Heat Transfer Properties of Pipe Insulation*, deals with the measurement of the heat transfer properties in steady state of pipe insulation. To perform this test, a tube device with a protected end or with a calibrated end is used. The protected end device is a primary method, while the calibrated end method is comparable, but not identical to that proposed by ISO 8497, *Thermal insulation - Determination of steady-state thermal transmission properties of thermal insulation for circular pipes*. The thermal properties determined by this test method include the effects

Table 2 - Summary of application conditions informed in the technical sheets of thermal insulation paints

	A	B	C	D	E
Application	Air spray, no airless	Airless	Airless brushing	Airless	Air spray / airless
Environment temperature	40 °C max.	(15 to 59) °C	(10 to 49) °C	above 10 °C	(10 to 43) °C
Surface temperature	Above 15.5 °C and +3 °C above dew point. T max. 149 °C	(15 to 148) °C	(10 to 177) °C	Above 10 °C and +3 °C above dew point	(10 to 121) °C
Relative humidity, RU (max.)	85 %	–	85 %	80 %	80 %
Wet thickness máx./coat (µm)	600	500	610	641	875 to 1000
Thickness for personal protection with hot surface at 177 °C (µm)	3048µm (7 coats)	4500 (9 coats)	2000 to 2500 (4 to 5 coats)	3000 µm (4 to 5 coats)	889 to 1016 (2 coats)
Curing time	48 h (RU 50 %)	(48 to 60) h	12 h	36 h	24 h
Interval between coats	20 °C: 6 h 30 °C: 3 h	2 h (RU 10 % to 30 %) 3 h (RU 50 %) 3.5 h (RU 70 %), 4 h (RU > 70 %)	2 h at 25 °C and 50 % RU	3 h (RU till 50 %)	5 h
Suggestion for anticorrosive primer	✓	Not necessary	–	✓	✓

Table 3 - Thermal properties informed in the technical sheets of thermal insulation paints

	A	B	C	D	E
Operation temperature	Till 177 °C	Till 190 °C	(-62 to 177) °C	Till 177 °C	(-51 to 176) °C. Avoid temperatures > than 93 °C in first hour.
Thermal conductivity	-	0.0698 W/(m*K) ASTM C177	0.097W/(m*K) ASTM C335	0.1W/(m*K) ASTM C518	At 23 °C: 0.0952 W/(m*K) At 50 °C: 0.0952 W/(m*K) At 149 °C: 0.1099W/(m*K) ASTM C177
Thermal Emissivity	-	0.14 a 0.18 Calculated ASTM C1371	-	-	0.85 ASTM E408
Reflexivity	-	0.85 ASTM C1371	-	0.803 ASTM E903	-
Transmissivity	-	0.0 calculated	-		-
Absorption	-	0.15 calculated	-	0.197 ASTM E903	-
Reflection UV	-	99.9 % ASTM G154	-	-	-

of adjustment and bonding, they are not true properties of the material. They are slightly different from the properties obtained in apparently similar material in flat form, using the protected hot plate, as will be seen in the ASTM C177 standard, or through the heat flow measuring device, as will be seen in the ASTM C518 standard.

ASTM C117, *Standard Test Method for Steady-State Heat Flux Measurements and Thermal Transmission Properties by Means of the Guarded-Hot-Plate Apparatus*, deals with a test method that establishes the criteria for the laboratory measurement of heat flow in steady state, through flat and homogeneous samples, when their surfaces are in contact with solid and parallel limits maintained at constant temperatures, using a protected heated plate apparatus. It is a method comparable to that described by ISO 8302, *Thermal insulation - Determination of steady-state thermal resistance and related properties - Guarded hot plate apparatus*. The steady-state heat transmission through thermal insulation is not easily measured, even at room temperature. This is because the transmission of heat through a sample occurs through any of the three modes (radiation, conduction and convection), or all of them. It is possible that any heterogeneity or anisotropy in the sample requires special experimental precautions to measure this heat flow. In some cases, it may take hours or even days to reach the thermal steady state. No protection system can be built to force heat to pass only through the test area of the insulating sample being measured. It is possible that the moisture content in the material causes transient behavior. It is also possible that physical or chemical changes in the material over time, or with the environmental condition, may permanently alter the sample. With this method, it is possible to use large sample areas. With the large areas, statistical representation of the heterogeneities intrinsic to the coatings in terms of thickness and microstructure is guaranteed. Thus, the values obtained for thermal conductivity must be more consistent with the actual conditions of application and use of the products.

The technical standard ASTM C518, *Standard Test Method for Steady-State Thermal Transmission Properties by Means of the Heat Flow Meter Apparatus*, deals with a test method that covers the measurement of steady-state thermal transmission through samples of flat plates using a heat flow meter. The heat flow meter is widely used because it is relatively simple in concept, fast and applicable to a wide range of test samples. The accuracy of the heat flow meter is excellent, as long as the calibration is performed within the expected heat flow range. This means that the calibration should be performed with similar types of materials, thermal conductance, thicknesses, average temperatures and temperature gradients, as expected for the test samples. The heat flow meter establishes a one-dimensional steady-state heat flow through a test sample between two parallel plates at constant but different temperatures.

Comparing the ASTM C177 and ASTM C518 standards, the measurements of the thermal properties of the material through the protected hot plate, ASTM C177 provide absolute results, while the properties obtained by the heat flow meter, ASTM C518, are relative, that is, the measurements have to be previously calibrated. This difference suggests that the ASTM C117 standard is preferable to the ASTM C518 standard. However, the difference in the value of the equipment in the two cases makes the analysis not so simplistic. The equipment that provides results according to the ASTM C117 standard is much more expensive than those suggested in the C518 standard. Consequently, the C518 method is more accessible. In addition, to being practical and economical, it is widely used worldwide for its speed, simplicity and precision. In this case, a sample is placed between two plates with controlled temperatures. These plates establish a temperature difference (ΔT) in the sample. The sample thickness (L) is defined to correspond to the actual dimension of use. The resulting heat flow (Q/(t.A) from the steady-state heat transfer through the sample is measured making it possible to determine the thermal conductivity K:

$$K = \frac{Q}{tA}\frac{L}{\Delta T}$$

In this section, emphasis was placed on the property of thermal conductivity. However, the other thermal properties (emissivity, reflectivity and absorptivity) can provide

Table 4 - Anti-corrosion properties informed in the technical sheets of thermal insulation paints

	A	B	C	D	E
Painting system	-	-	Primer + Insulation + Topcoat	-	Primer +Insulation
Test	-	ASTM B117	ASTM D5894	-	ASTM D5894
	-	6000 h	3024 h (9 cycles)	-	2016 h
Result	-	Excellent >2100 h	Blisters (ASTM D714): 10 Rusting (ASTM D610): 9 Scribe Creepage (ASTM D1654): 10	-	 No rusting No blister
Adhesion	-	-	ASTM D 3359: 5A ASTM D 4541: 360 psi	-	-
Permeability		4.98 perms ASTM 1653-03			

important complementary information for the performance of the insulators. In this context, Demuner [10] proposes the use of thermography to determine these properties. The evaluation of the procedure is in progress. One of the conventional methods for determining these properties is suggested by ASTM E903 - *Standard Test Method for Solar Absorptance, Reflectance, and Transmittance of Materials Using Integrating Spheres*. The advantage of the method proposed by Demuner [10] is that the evaluation can be made in the environment where the paint is applied, without the need for physical contact with the structure or preparation of samples.

Table 4 shows the anti-corrosion properties reported in the technical datasheets. With regard to aging, two suppliers show results of anti-corrosion performance in a cyclic test suggested by Standard ASTM D5894, but with a complete scheme containing anti-corrosion paints. Only one supplier includes the corrosion test according to ASTM B117 with the thermal insulation paint alone. Only one supplier shows permeability results. No supplier shows the variation of thermal properties after the aging tests. Based on the above discussion, standardized aging tests with thermal shocks/cycles can be very appropriate to characterize not only anti-corrosion performance, but also, variation of mechanical properties and, above all, thermal properties.

Conclusions

Thermal insulation paints represent an advance with technical and economic advantages for structures operating up to approximately 200 °C, in atmospheric exposure. However, the large user has difficulty in establishing technical specifications due to the heterogeneity, or even lack of information about the thermal properties of these paints and their variation with the aging inherent to the service conditions. Corrosion tests in the laboratory, involving temperature variations, can assist in the definition of complementary anti-corrosion schemes. Additionally, they can be a tool for characterizing the degradation of mechanical and thermal properties of insulating paints, enabling conservative dimensioning of the thicknesses required for insulation. With this more holistic approach to performance, data sheets can become more homogeneous and robust in data, creating a culture of more grounded use of these products. The adoption of this approach in technical specifications for large users will certainly be a great stimulus for this transformation.

References

1. Shong, D., Corrosion/2017, paper no. 8876, (Houston, TX: NACE International, 2017).

2. Li, Y., Ge, D., Yang, L., Zhao, J., Journal of Non-Crystalline Solids, **355** (2009) 2610.

3. Achar, S., Procopio, L. J., Journal of Protective Coatings and Linings, **30** (3) (2013) 48.

4. Kang, Q., Bao, Y., Li, M., Ma, J., Progress in Organic Coatings, **112** (2017) 153.

5. Yang, H., Jiang, Y., Liu, H., Xie, D., Wan, C., Pan, H., Jiang, S., Journal of Colloids and Interface Science, **530** (2018) 163.

6. Silva, T.C., Mallarino, S., Touzain, S., Margarit-Mattos, I.C.P., Electrochimica Acta, **318**(20) (2019) 989.

7. Geary, W., Case Studies in Engineering Failure Analysis, **1** (2013) 249.

8. Miyashita, J., Corrosion/2017, paper no. 9296, (Houston, TX: NACE International, 2017).

9. Baer, A., Corrosion/2018, paper no. 10671, (Houston, TX: NACE International, 2018).

10. Demuner, J.C.D., Fardin, J.F., Muniz, P.R., Gomes, L.C., Proceedings of the XXXVI Iberian Latin-American Congress on Computational Methods in Engineering, CILAMCE 2015, Ney Augusto Dumont (Editor), ABMEC, Rio de Janeiro, RJ, Brazil, November 22-25, 2015

Detection and enumeration of diverse sulfate-reducing and thiosulfate reducing microbial species using thin-film culture device technology

Evan Brutinel[a], Benjamin Wilson[a], Sergio Filho[b], Peter Gorman[c]

[a] PhD, Research Specialist - 3M Company, St. Paul, MN
[b] Application Engineer – 3M Brazil
[c] Application Engineer - 3M Company, St. Paul, MN

Abstract

Specific groups of microorganisms have been linked to an increased risk for microbiologically influenced corrosion (MIC) and reservoir souring. Culture-based detection of corrosion associated microbes (e.g., sulfate reducing bacteria or SRB) remains a key aspect of industrial and oil field corrosion management. Unfortunately, growing these organisms in the field continues to be challenging as they can be difficult to grow using traditional microbiological methods (e.g., anaerobic culture bottles). Recently, a new thin-film culture device has become available for the detection and enumeration of SRBs and thiosulfate-reducing bacteria in surface, flowback, cooling, and produced waters. Here, the growth and enumeration of several strains is compared to that of currently available culture-based technologies. Importantly, representative species from several lineages were used to prevent biasing for one general type including members of the Deltaproteobacteria and Firmicutes. Thermophilic and halophilic strains were included, with incubation temperatures and solution salinities adjusted accordingly. Tests were inoculated, incubated, and scored in accordance with the NACE standard (serial dilution bottles) or per the manufacturer's instructions. The results indicate that the thin-film culture device recovers a wider variety of species and is able to accurately quantify bacterial number despite varying conditions for each strain.

Keywords: Microbiologically influenced corrosion, reservoir souring, sulfate reducing bacteria, NACE

Introduction

Microbiologically influenced corrosion (MIC) is widely recognized as a significant contributor to corrosion in the oil and gas industry (1, 2). Detection and accurate enumeration of microbial species associated with MIC is critical to determine the efficacy of routine biocide usage and to swiftly identify a problem if it occurs. Anaerobic serial dilution bottles are commonly used in conjunction with the most probable number (MPN) method to estimate bacterial populations in water samples (3). While bacterial numbers are often reported in order of magnitude according to "bottle turns", MPN estimations have an inherently large standard error due to stochastic events when repeatedly diluting the sample. For example, while 4 "bottle turns" is often reported as 10,000 bacteria per mL, the range for this result from a single dilution series is in fact 690 to 145,000 MPN/mL (3). Brutinel et. al. demonstrated this empirically by performing 16 replicate dilution series from the same water sample containing a lab strain of sulfate-reducing bacteria (SRB) commonly associated with MIC. Despite performing the experiment under ideal laboratory conditions, a wide range of results were returned spanning 3 orders of magnitude (4). Compounding the problem, serial dilution bottles require the operator to measure the total dissolved solids (TDS) of the sample and use a media with a similar TDS level. Commonly, the TDS level of a sample or set of samples is unknown prior to testing, requiring field personnel to stock up to 6 different TDS level bottles for each organism type to be tested. In the above-mentioned paper, Brutinel et. al. demonstrate the effect TDS mismatch can have on field samples. In one example a 3% TDS produced water sample was tested for SRB using 1% and 10% TDS modified Postgate B (MPB) serial dilution bottles. Using the MPN method the 1% bottles returned a result of 45,000 MPN/mL while the 10% bottles returned a result of 9.5 MPN/mL (4). This large difference in results could lead to very different actions from the asset owner, from no biocide treatment to aggressive over-treatment. Finally, to accurately enumerate bacterial populations, serial dilution bottles must culture every target organism in the sample, as the final dilution bottle to return a positive result must contain only a few bacteria. Strict anaerobes like SRB are notoriously difficult to grow in culture media, especially when robust growth is required to return a positive result in a 10 mL bottle.

Given the above limitations of serial dilution bottles and the MPN method, it should not be surprising that other methods of culture-based detection of MIC causing organisms have been devised. One of these methods, referred to in this manuscript as the time-to-result (TTR) method, will be further addressed. The TTR method typically uses only a single bottle or container with a growth medium inside. The water sample to be tested is added directly to the container and sealed, the container is incubated at a temperature close to that of the sample in question, and the operator records the amount of time it takes for the test to return a positive result. Similar to serial dilution bottles, the nature of the positive result varies depending on the target group of organisms, e.g. black FeS precipitate for SRB, color change based on pH for acid-producing bacteria (APB), etc. The time it takes for the test to return a positive result is inversely proportional to the number of target bacteria in the water sample because the test is essentially measuring metabolic output. In the case of SRBs, the higher concentration of SRBs in the original sample, the faster a threshold level of sulfide will be reached and produce a visible amount of FeS precipitate, indicating a positive test. Manufactures of TTR-style tests provide guidance on how many microorganisms per mL are present based on a timetable.

TTR style tests have a number of advantages as compared to serial dilution bottles. First, TTR-style tests used in the oil field are hydrated with the incoming sample. This has the advantage of eliminating the TDS matching step, as the sample provides the appropriate level of TDS for the test. Second, all of the target organisms that are being enumerated are present in

the sample. This reduces the reliance on robust growth from just a few organisms seen in the serial dilution method. Third, because a larger number of organisms are being grown in the same container, the TTR of this style of test is typically days or weeks shorter than that of serial dilution bottle. Finally, the single tube test is much easier to perform in the field and requires fewer consumables. Despite their obvious advantages, there remain two main concerns with TTR-style tests. First, TTR-style tests are typically not provided in a sealed anaerobic manner. While this contributes to the ease of use, as needles are not required, it means that a test which is aerobically inoculated must then grow strictly anaerobic bacteria. The anaerobic environment is presumably achieved when the other aerobic and facultative anaerobic bacteria in the sample consume the oxygen, but this contributes to the variability of the result as the number and identity of the bacteria will determine the speed at which the test becomes anaerobic. Second, there is a concern that varying growth rates of microorganisms will dramatically affect the accuracy of TTR-style tests. Microorganisms present in oil field waters represent a diverse set of species with vastly different growth temperatures and salinity requirements. In a TTR-style test, the concentration of faster growing organisms should be overestimated, while the concentration of slower growing organisms should be underestimated.

Recently, a new TTR-style test has become available for the enumeration of SRBs in oil field and industrial waters. The 3M Rapid SRB Detection pouch is a thin-film culture device consisting of plastic films that form a pouch with an SRB growth medium, as well as oxygen scrubbing and redox modifying chemistry, coated on the inside (Figure 1). Here, we assess the ability of this new test to accurately enumerate a wide variety of SRB species requiring vastly different growth temperatures and salinities.

Methodology

Materials: 3M™ Rapid SRB Detection Pouches and Butterfield's buffer dilution blanks were obtained from 3M Company (St. Paul, MN). Bacterial strains were obtained from Microbiologics Inc. (St. Cloud, MN), the American Type Culture Collection (ATCC; Manassas, VA) or the Leibniz Institute DSMZ (Germany). Starkey's agar was obtained from HiMedia Laboratories (West Chester, PA) and prepared per manufacturer's instructions. Chemicals for media preparation were obtained from Millipore-Sigma (St. Louis, MO). Sea salt mix was obtained from Instant Ocean (Blacksburg, VA). The anaerobic culture system for agar plates was obtained from Becton Dickinson (BD GasPak™ EZ pouch system†, Franklin Lakes, NJ). Modified Postgate B (MPB) anaerobic serial dilution bottles were obtained from Biotechnology Solutions LLC (Houston, TX).

Culture Methods: Cultures of *Desulfovibrio desulfuricans* ATCC #29577 and *Desulfovibrio vulgaris* ATCC #29579 were grown in a modified Starkey's Broth (tryptone 15 g/L, soy peptone 5 g/L, sodium chloride 5 g/L, magnesium sulfate heptahydrate 2 g/L, ammonium sulfate 0.6 g/L, 60% sodium lactate 4.0 mL/L,

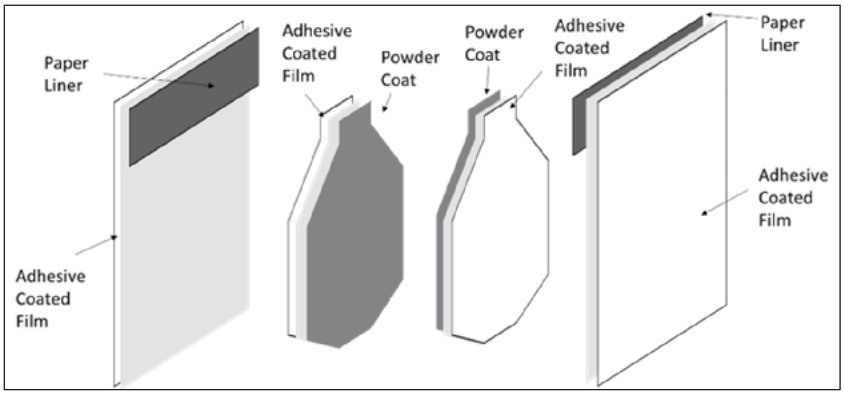

Figure 1. Exploded of the components that make up the 3M™ Rapid SRB Detection Pouch.

final pH (at 25°C) 7.3±0.1) in Balch tubes under an anaerobic head space (N_2) at 30°C. Dilution of both strains for inoculation was done in sterile aerobic Butterfield's Buffer. Cultures of *Desulfovibrio alaskensis* ATCC #14563 were grown in 2.5 % sodium chloride modified sodium lactate for sulfate reducers medium (yeast extract 1 g/L, magnesium sulfate heptahydrate 1 g/L, ammonium chloride 0.4 g/L, potassium phosphate dibasic 0.01 g/L, sodium chloride 25 g/L, sodium ascorbate 0.1 g/L, sodium lactate 4 mL of 60% stock, final pH (at 25°C) 7.3±0.1) in Balch tubes under an anaerobic head space (N_2) at 37°C. Dilution of *D. alaskensis* for inoculation was done in sterile aerobic Butterfield's Buffer amended with 36 g/L seas salt. Cultures of *Desulfovibrio gracilis* ATCC #BAA-904 were grown in ATCC Medium 2465 (ATCC.org) in Balch tubes under an anaerobic head space (N_2) at 37°C. Dilution of *D. alaskensis* for inoculation was done in sterile aerobic Butterfield's Buffer amended with 50 g/L sodium chloride. Cultures of *Thermoanaerobacter brockii subsp lactiethylicus* DSM-9801 were grown in DSMZ Medium 520 with strain-specific modifications (DSMZ.de) in Balch tubes under an anaerobic head space (80% N_2 / 20% CO_2) at 60°C. Dilution of *T. brockii* for inoculation was done in sterile aerobic Butterfield's Buffer. Cultures of *Desulfotomaculum nigrificans* ATCC #7946 were grown in ATCC Medium 1249 (ATCC.org) in Balch tubes under an anaerobic head space (N_2) at 45°C. Dilution of *D. nigrificans* for inoculation was done in sterile aerobic Butterfield's Buffer. Cultures of *Clostridium sporogenes* ATCC#11437 were grown in tryptic soy broth (TSB) in Balch tubes under an anaerobic head space (N_2) at 37°C. Dilution of *C. sporogenes* for inoculation was done in sterile aerobic Butterfield's Buffer.

Reference counting: Enumeration of *D. vulgaris*, *D. desulfuricans*, *D. alaskensis*, and *T. Brockii* was achieved by plating dilutions on Starkey's Agar, incubating in an anaerobic box at the above culturing temperatures, and counting colonies. *D. nigrificans* and *C. sporogenes* were similarly enumerated on sulfite agar and TSB agar, respectively. Enumeration of *D. gracilis* was performed using 5%TDS MPB serial dilution bottles because a solid media capable of producing countable colonies could not be found. Dilution series were inoculated in triplicate per the NACE standard (3) and the MPN method was used to calculate MPN/mL (Bacteriological Analytical Manual, FDA.gov).

Time Lapse Photography and Data Analysis: 3M Rapid SRB Detection Pouches were inoculated (3 mL) and sealed according to the manufacturer's instructions (Figure 2) with bacterial cultures diluted from stocks as described above. Determination of bacterial concentration using time-lapse photography was performed as previously described (4). Briefly,

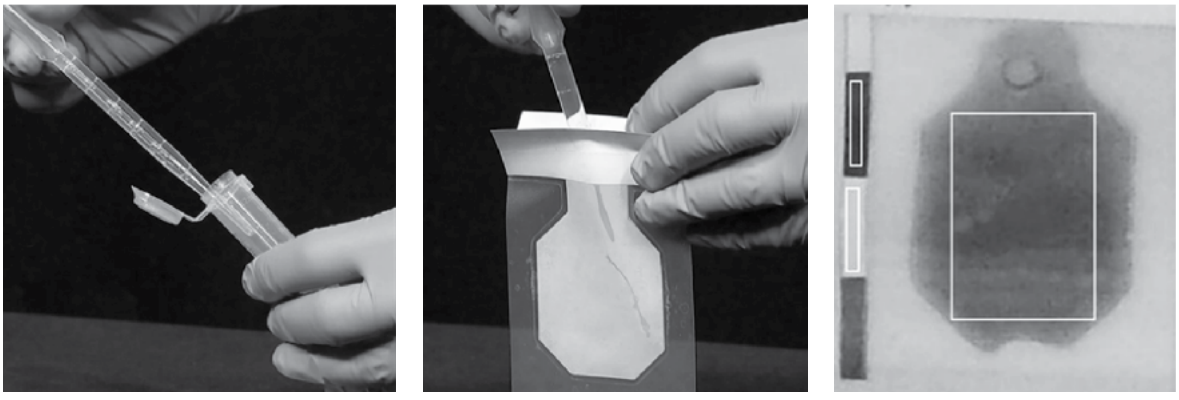

Figure 2. Inoculation, incubation, and time-lapse photography of the 3M Rapid SRB Detection Pouch. 3 mL of sample is drawn up aerobically (Panel 1) and injected into the lumen of the pouch (Panel 2). The white paper tabs are removed, and the pouch is sealed with the now exposed adhesive (not shown). During incubation, for the purposes of time-lapse photography, pouches were affixed to a board next to black/white standards which were used to normalize the color change of the pouch (Panel 3, white boxes)

Pouches were placed next to black/white color standards (Figure 2, panel 3), incubated at the above indicated temperature, and a time lapse camera imaged the pouches every 5 minutes. Image analysis software was used to assign a black/white value to each pouch at each time point relative to the adjacent black/white standard. The black/white values for each pouch were then plotted versus time to determine the TTR of each pouch. For any given bacterial concentration, at least 4 replicate pouches were inoculated.

Results

Growth of SRB in the 3M Rapid SRB Detection Pouch, similar to serial dilution bottles, is indicated by the appearance of a black ferrous sulfide precipitate. The higher the concentration of SRB in the sample, the faster the black precipitate appears. To validate that the TTR of the 3M Rapid SRB Detection Pouch consistently demonstrates a linear correlation with the logarithmic concentration of SRB in the sample, dilutions of *D. desulfuricans* and *D. vulgaris* spanning 6 orders of magnitude were assayed using the pouch and time-lapse photography (4). The 3M Rapid SRB Detection Pouch returned predictable and reproducible results dependent on starting SRB concentration (Figure 3).

D. desulfuricans and *D. vulgaris* are two closely related species of Deltaproteobacteria that grow at similar temperatures and salinities. It is therefore not surprising that the TTR is highly similar for both organisms in the 3M Rapid SRB Detection Pouch. Four additional SRB species and one thiosulfate reducing bacteria were chosen for analysis (Table 1). Importantly, these species were chosen because (1) some are more distantly related to the *Desulfovibrios* and include representatives from the Phylum Firmicutes, (2) they include more halophilic species with optimal salinities of 3% and 5%, and (3) they include more thermophilic species with optimal growth temperatures of 37, 45, and 60°C.

Inoculums for experimentation were generated by performing 10-fold dilution series aerobically in sterile Butterfields buffer with stock cultures of the bacterial strains in Table 1. Dilution buffers were amended with salt for the halophilic strains. 3M Rapid SRB Detection Pouches were inoculated as shown in Figure 2 and incubated at the temperature indicated in Table 1. Time-lapse photography was used to determine TTR for each concentration of each organism. To determine the actual number of bacteria in each sample, dilutions were plated on solid media and colonies were counted. *D. gracilis* was unable to form countable colonies on solid media so MPB serial dilution bottles, performed in triplicate, were used in conjunction with the MPN method to determine bacterial concentration. The results of the TTR experiments are shown in Figure 4.

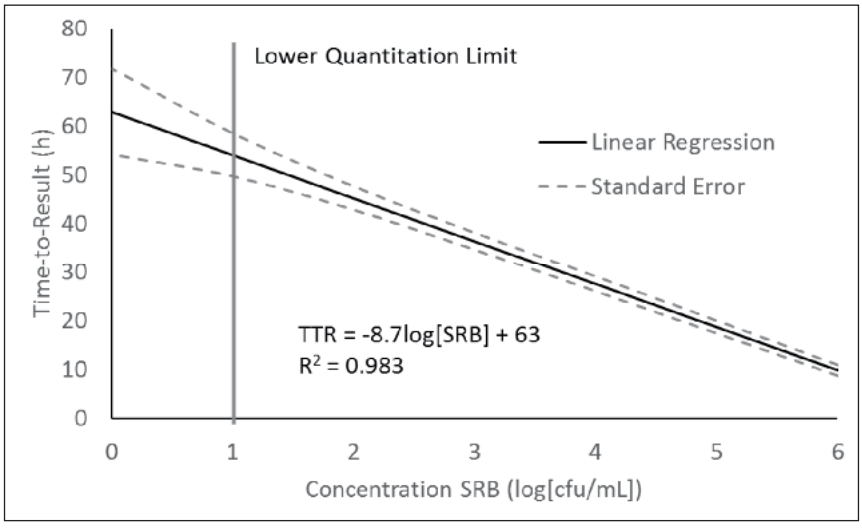

Figure 3: Correlation between TTR and starting SRB concentration of D. desulfuricans *and* D. vulgaris. *The lower quantitation limit (grey vertical line) was set at the concentration above which 100% of the pouches were calculated to have an SRB concentration within 1 log unit of the known value (counts from Starkey's Agar plates) and 96% within 0.5 log units (4).*

Table 1 - Bacterial species tested in the 3M Rapid SRB Detection Pouch.

SRB species	Numer	TDS (%)	Temp (°C)
Desulfovibrio desulfuricans	ATCC #29577	1	30
Desulfovibrio vulgaris	ATCC #29579	1	30
Desulfovibrio alaskensis	ATCC #14563	3	37
Desulfovibrio gracilis	ATCC #BAA-904	5	37
Thermoanaerobacter brockii	DSM-9801	1	60
Desulfotomaculum nigrificans	ATCC #7946	1	45
Clostridium sporogenes	ATCC#11437	1	37

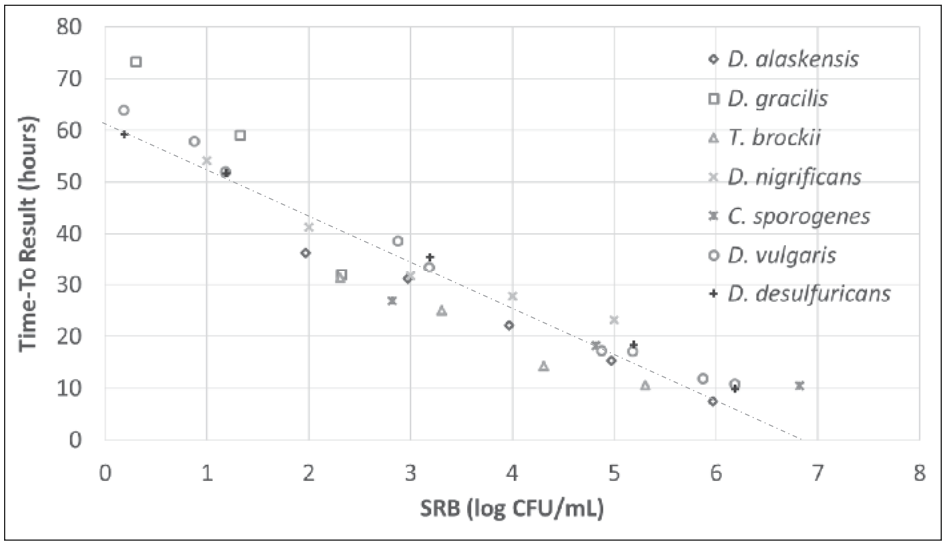

Figure 4. Time-to-result for various concentrations of seven species of SRB and thiosulfate reducing bacteria.

Similar to the results obtained with D. vulgaris and D. desulfuricans alone, the 3M Rapid SRB Detection Pouch returned predictable and reproducible results dependent on starting SRB concentration.

Figure 3 shows the equation that relates bacterial concentration to TTR for *D. desulfuricans and D. vulgaris* as TTR = -8.7 * log[CFU/mL SRB] + 63 with an R^2 value of 0.983. When calculated using the results plotted in Figure 4, the aggregated data produces a highly similar line described by TTR = -8.9 * log[CFU/mL] + 61 with an R^2 value of 0.903. ANOVA analysis was performed using the data plotted in Figure 4 to determine if bacterial concentration, bacterial identity (species), or both contributed significantly to the TTR of a given sample. Bacterial concentration was found to be highly significant (p-value <0.000) while bacterial identity was not found to be significant (p-value = 0.115). In addition, bacterial concentration was responsible for 70.2% of the TTR value while bacterial identity was responsible for only 27.5% of the TTR value, with the caveat that bacterial identity was not found to be significant. 2.3% of the TTR value was not explained by the model.

Conclusions

TTR-based tests for enumerating microbial populations offer many advantages over traditional culture methods. The operator monitors the test and records the amount of time between inoculation and a positive result. Test

manufactures provide guidance, usually based on laboratory studies with one microbial strain, that relates the TTR to a concentration of microbes. Given the wide diversity of microbial species, guidance based on a single microbial species may not capture the whole picture and test kits should be validated with a wide variety of strains and field samples to ensure accurate and repeatable reporting. In this study, the ability of the 3M Rapid SRB Detection Pouch to accurately estimate the concentration of SRBs with a variety of temperature and TDS requirements was assessed. The data show that the test returned predictable and reproducible results dependent on starting SRB concentration (Figure 3) regardless of SRB species. ANOVA analysis showed that the primary contributor to the result was SRB concentration (70.2%) with SRB species playing a minor role (27.5%) that was not statistically significant (p-value = 0.115). These results are consistent with previous studies comparing the estimation of SRB concentration by the 3M Rapid SRB Detection Pouch to serial dilution bottles (4) and molecular microbiology methods (MMMs)(5).

In this manuscript the TTR for the 3M Rapid SRB Detection Pouch was determined using time-lapse photography. While this was convenient for lab studies, the test is intended for use in the field. The test is provided with a paper-based guide that allows an operator to compare the color of the pouch to that of standards. While the paper guide was designed based solely on the data shown in Figure 3, the results presented in Figure 4 suggest that it will be accurate for a variety of SRB species.

One of the main advantages of TTR-style tests is the ease of use, particularly the elimination of needles typically used for serial dilution bottles. This reduces the burden on an operator for bringing material to the field and can save large amounts of storage space as well in offshore applications. This does present a problem however, in that TTR-based tests are inoculated aerobically but must culture strictly anaerobic microbes. In this study, in addition to 3M Rapid SRB Detection Pouches and serial dilution bottles, three different TTR-style tests were purchased and inoculated / incubated according to the manufacturer's instructions with the same samples. Without exception, these other TTR-style tests either did not return a positive result, or significantly underreported the concentration of SRB in the sample. As discussed in the introduction, most TTR-style tests rely on the aerobic and facultative-anaerobic microorganisms in a water sample to remove the oxygen. Inoculation with a single SRB species is not the intended use of these products so the above results are not surprising. It does suggest that TTR-style tests that rely on other microbes will be sensitive to the number and identity of non-target microbes in a sample, increasing variability of the result. The 3M Rapid SRB Detection Pouch contains oxygen scrubbing and redox modifying chemistry that is activated by the addition of the water sample. Within 15 minutes of inoculation, the 3 mL sample is rendered anaerobic with a reduction potential below that which is required for culturing strictly anaerobic bacteria (-200 mv) (4). This has an added advantage of reducing competition for media components by non-target bacteria, reducing variability further.

Acknowledgements

We wish to thank N. Reierson for help preparing this manuscript.

References (Unedited)

1. TL. Skovhus, et al. (2017) Microbiologically Influenced Corrosion in the Upstream Oil and Gas Industry, 1st Ed. (Boca Raton, FL, CRC Press).

2. N. Youssef, et al. (2009) Microbial processes in oil fields: cuprits, problems, and opportunities, Adv Appl Microbiol. 66:141.

3. NACE TM0194-2014 (Latest Version), "Field Monitoring of Bacterial Growth in Oil and Gas Systems" (Houston, TX: NACE)

4. ED. Brutinel, B. Wilson, and K. Gangelhoff. (2019) Evaluation of a self-contained, anaerobic environment-generating culture device for detection of sulfate-reducing bacteria. NACE Corrosion 2019 (NACE; Houston, TX)

5. ED. Brutinel, B. Wilson, N. Reierson, K. Yarina, P. Gorman. Comparative study of a novel thin-film culture device, serial dilution bottles, and 16S metagenomics for enumeration of sulfate reducing bacteria in field samples. International Symposium on Applied Microbiology and Molecular Biology in Oil Systems 7 (ISMOS7). (Halifax, NS)

ABRACO

EMPRESAS ASSOCIADAS

A IDEAL SOLUÇÕES ANTICORROSIVAS EIRELI ME
www.aideal.com.br/site/

ADVANCE TINTAS E VERNIZES LTDA.
www.advancetintas.com.br

AKZO NOBEL LTDA - DIVISÃO COATINGS
www.akzonobel.com/international

APERAM
www.brasil.aperam.com

BBOSCH GALVANIZAÇÃO DO BRASIL LTDA.
www.bbosch.com.br

CEPEL - CENTRO PESQ. ENERGIA ELÉTRICA
www.cepel.com.br

COVESTRO INDÚSTRIA E COMÉRCIO DE POLÍMEROS LTDA
www.covestro.com

DE NORA DO BRASIL LTDA.
www.denora.com

DEEPWATER DO BRASIL ENGENHARIA LTDA.
www.stoprust.com

FURNAS CENTRAIS ELÉTRICAS S/A
www.furnas.com.br

G P NÍQUEL DURO LTDA.
www.grupogp.net

HITA COMÉRCIO E SERVIÇOS LTDA.
www.hita.com.br

ICM METAIS
http://site.icm.ind.br/

IEC INSTALAÇÕES E ENGª DE CORROSÃO LTDA.
www.iecengenharia.com.br

INSTITUTO SENAI DE INOVAÇÃO
EM ELETROQUÍMICA – ISI – EQC
www.senaipr.org.br/tecnologiaeinovacao/nossarede/eletroquimica/

INSTITUTO NACIONAL DE TECNOLOGIA – INT
www.int.gov.br

JOTUN BRASIL IMP. EXP. E IND. DE TINTAS LTDA.
www.jotun.com

PETROBRAS S/A - PETRÓLEO BRASILEIRO / CENPES
www.petrobras.com.br

PETROBRAS TRANSPORTES S/A - TRANSPETRO
www.transpetro.com.br

PRESSERV DO BRASIL LTDA.
www.cortecpresserv.com.br

PROMAR TRATAMENTO ANTICORROSIVO LTDA.
www.promarpintura.com.br

RENNER HERRMANN S/A
www.renner.com.br

SACOR SIDEROTÉCNICA S/A
www.sacor.com.br

SMARTCOAT ENGENHARIA EM REVESTIMENTOS LTDA.
www.smartcoat.com.br

TBG - TRANSP. BRAS. GASODUTO BOLÍVIA – BRASIL
www.tbg.com.br

TECHNIQUES SURFACES DO BRASIL LTDA.
www.tsbrasil.srv.br

TECNOFINK LTDA.
tecnofink.com

TINÔCO ANTICORROSÃO LTDA.
www.tinocoanticorrosao.com.br

W&S SAURA LTDA.
wsequipamentos.com.br

ZERUST PREVENÇÃO DE CORROSÃO LTDA.
www.zerust.com.br

ZINCOLIGAS INDÚSTRIA E COMÉRCIO LTDA.
www.zincoligas.com.br

ASSOCIAÇÃO BRASILEIRA DE CORROSÃO

Av. Venezuela, 27 • Sl. 412/418 • Centro • Rio de Janeiro • CEP 20081-311

(21) 2516-1962 • www.abraco.org.br

Facebook: facebook.com/abraco.oficial

LinkedIn: linkedin.com/in/abraco

Instagram: @abraco_br

Youtube: Associação Brasileira de Corrosão

SETORES

Associados: secretaria@abraco.org.br

Biblioteca: biblioteca@abraco.org.br

CB-43: cb43@abraco.org.br

Comunicação: marketing@abraco.org.br

Eventos: eventos@abraco.org.br

Financeiro: financeiro@abraco.org.br

Gerência Geral: gerenciageral@abraco.org.br

Presidência: presidencia@abraco.org

Qualificação e Certificação: qualificacao@abraco.org.br

Treinamentos: cursos@abraco.org.br